

1 *Review*

2 **Instability and Convection in Rotating Porous Media:** 3 **A Review**

4 **Peter Vadasz** ^{1,*}

5 ¹ Department of Mechanical Engineering, Northern Arizona University; e-mail: Peter.Vadasz@nau.edu

6 * Correspondence: Peter.Vadasz@nau.edu; Tel.: +1-928-523-5251

7 Academic Editor: Andrew S. Rees, Antonio Barletta

8 Received: **date**; Accepted: **date**; Published: **date**

9 **Abstract:** A review on instability and consequent natural convection in rotating porous media is
10 presented. Taylor-Proudman columns and geostrophic flows exist in rotating porous media just
11 the same as in pure fluids. The latter leads to a tendency towards two-dimensionality. Natural
12 convection resulting from density gradients in a gravity field as well as natural convection
13 induced by density gradients due to the centripetal acceleration are being considered. The former
14 is the result of gravity-induced buoyancy, the latter is due to centripetally-induced buoyancy. The
15 effect of Coriolis acceleration is also discussed. Linear stability analysis as well as weak nonlinear
16 solutions are being derived and presented.

17

18 **Keywords:** Rotating Flows; Porous Media; Natural Convection; Instability; Taylor-Proudman
19 column; Centrifugal Buoyancy, Coriolis Acceleration.

20

21 **1. Introduction**

22 The research into the effects of rotation on the flow and transport phenomena in porous media
23 is driven by the fundamental scientific significance as well as by engineering and geophysical
24 applications. To be specific, one refers to flows in porous geological formations subject to earth
25 rotation, to the flow of magma in the earth mantle close to the earth crust (Fowler [1]) as
26 geophysical applications. The food process industry, chemical process industry, centrifugal
27 filtration processes, and rotating machinery are examples of engineering applications.

28 For example, packed bed mechanically agitated vessels are being used in the food processing
29 and chemical engineering industries in batch processes. The packed bed consists of solid particles
30 or fibers of material, which form the solid matrix while fluid flows through the pores. As the solid
31 matrix rotates, due to the mechanical agitation, a rotating frame of reference is a necessity when
32 investigating these flows. The role of the flow of fluid through these beds can vary from drying
33 processes to extraction of soluble components from the solid particles. Two examples of such
34 processes are the molasses subject to centrifugal crystal separation in the sugar milling industry and
35 the extraction of sodium alginate from kelp. Additional industrial applications are being presented
36 in Vadasz [2,3,4], Nield and Bejan [5,6], and Bejan [7] in comprehensive reviews of the
37 fundamentals of heat convection in porous media.

38 With the emerging utilization of the porous medium approach in non-traditional fields,
39 including some applications in which the solid matrix is subjected to rotation (like physiological
40 processes in human body subject to rotating trajectories, cooling of electronic equipment in a
41 rotating radar, cooling of turbo-machinery blades, or cooling of rotors of electric machines) a
42 thorough understanding of the flow in a rotating porous medium becomes essential. Its results can
43 then be used in the more established industrial applications like food processing, chemical

44 engineering or centrifugal processes, as well as to the less traditional applications of the porous
45 medium approach.

46 The fundamental equations and assumptions applicable to single-phase convective heat
47 transfer were presented by Dagan [8], Acharya [9]. A review of the effects of rotation on heat
48 transfer in general was presented by Wiesche [10].

49 Reviews of the fundamentals of flow and heat transfer in rotating porous media were
50 presented by Vadasz [2, 3, 4, 11, 12, 13, 14, 15].

51 No reported results were found on isothermal flow in rotating porous media prior to 1994.
52 Research of a pioneering nature on natural convection in rotating porous media were reported by
53 Rudraiah et al [16], Patil and Vaydianathan [17], Jou and Liaw [18, 19], and Palm and Tyvand [20].
54 Nield [21] found that the effect of rotation on convection in a porous medium attracted limited
55 interest in a comprehensive review of the stability of convective flows in porous media.

56 The fact that isothermal flow in homogeneous porous media following Darcy law is
57 irrotational and hence the effect of rotation on this flow is insignificant contributed to the limited
58 interest for this type of flow. However, for natural convection in a non-isothermal homogeneous
59 porous medium or for a heterogeneous medium with spatially dependent permeability the flow is
60 not irrotational anymore, and therefore the effects of rotation become significant. More recent
61 interest in this type flow, during the past three decades, led to an increased number of publications.
62 For example, Nield [22], Auriault et al [23, 24], Govender [25, 26], Havstad and Vadasz [27], Vadasz
63 and Havstad [28], Govender and Vadasz [29, 30, 31, 32], Vadasz [2, 3, 4, 11, 12, 13, 14, 15, 33, 34, 35,
64 36, 37, 38, 39, 40, 41, 42], Vadasz and Govender [43, 44], Vadasz and Heerah [45], Vadasz and Olek
65 [46], Bhaduria [47], Malashetty, Pop, Heera [48], Vanishree and Siddheshwar [49], Agarwal et al
66 [50], Bhaduria et al [51], Agarwall and Bhaduria [52], Malashetty et al [53], Malashetty and
67 Swamy [54], Rana and Agarwal [55], Yadav et al [56], Rashidi et al [57], Makinde et al [58],
68 Straughan [59], Lombardo and Mulone [60], Falsaperla, Mulone and Straughan [61, 62], Falsaperla,
69 Giacobbe and Mulone [63], Capone and De Luca [64], Capone and Rionero [65], Capone and De
70 Luca [66].

71

72 2. Governing Equations

73 The equations governing the flow and heat transfer in rotating porous media are presented in a
74 dimensionless form subject to the assumptions of constant angular velocity of rotation, Boussinesq
75 approximation (Boussinesq [67]), and local thermal equilibrium (LTE or Lotheq). The latter implies
76 that the difference in the local temperature between the solid and fluid phases in the porous
77 medium is insignificantly small and can be neglected. Boussinesq approximation [67] applicable to
78 buoyancy flows states that the density is constant in all terms of the governing equations except the
79 buoyancy terms in the momentum equation. The notation being used refers to symbols having an
80 asterisk as dimensional, while symbols without an asterisk represent dimensionless quantities,
81 except symbols carrying the subscript "c" representing characteristic values, or the subscript "o"
82 representing reference values, both being dimensional. The continuity equation is presented in the
83 form

$$84 \nabla \cdot \mathbf{V} = 0 \quad (1)$$

85 where $\mathbf{V} = u \hat{\mathbf{e}}_x + v \hat{\mathbf{e}}_y + w \hat{\mathbf{e}}_z$ is the filtration velocity vector presented in Cartesian coordinates,
86 u, v, w are the components of the the filtration velocity vector in the x, y, z directions,
87 respectively, and $\hat{\mathbf{e}}_x, \hat{\mathbf{e}}_y, \hat{\mathbf{e}}_z$ are unit vectors in the x, y, z directions, respectively. The operator $\nabla \cdot$
88 is the divergence operator defined in the form $\nabla \cdot \equiv [\hat{\mathbf{e}}_x \partial(\)/\partial x + \hat{\mathbf{e}}_y \partial(\)/\partial y + \hat{\mathbf{e}}_z \partial(\)/\partial z]$.

89 The momentum transport in porous media is governed primarily by the Darcy law, which is
90 presented in the rotating frame of reference of the solid matrix in the following dimensionless form

$$91 \mathbf{V} = -N_p \nabla p + Fr \rho \hat{\mathbf{e}}_g - Cn \rho \hat{\mathbf{e}}_\omega \times (\hat{\mathbf{e}}_\omega \times \mathbf{X}) - \frac{\rho}{Ek_\Delta} \hat{\mathbf{e}}_\omega \times \mathbf{V} \quad (2)$$

92 where four dimensionless groups emerged, i.e. a pressure number N_p (equivalent to a porous
 93 media Euler number where $\mu_* l_c / K_*$ replaces $\rho_o u_c$), a porous media Froude number Fr , a
 94 centrifugal number Cn , and a porous media Ekman number Ek_Δ defined in the form

$$95 \quad N_p = \frac{K_* \Delta p_c}{\mu_* u_c l_c}, \quad Fr = \frac{g_* K_*}{v_* u_c}, \quad Cn = \frac{K_* \omega_*^2 l_c}{v_* u_c}, \quad Ek_\Delta = \frac{\phi v_*}{2 \omega_* K_*} \quad (3)$$

96 and where K_* and ϕ are the permeability and the porosity of the porous matrix, respectively, μ_*
 97 is the dynamic viscosity, ρ_o is a constant reference value of the fluid density used to convert the
 98 density into a dimensionless form, $v_* = \mu_* / \rho_o$ is the kinematic viscosity of the fluid, ω_* is the
 99 constant angular velocity of rotation, p and ρ are the dimensionless pressure and density,
 100 respectively, \hat{e}_g is a unit vector in the direction of the gravity acceleration, \hat{e}_ω is a unit vector in
 101 the direction of the angular velocity of rotation, and $\mathbf{X} = x\hat{e}_x + y\hat{e}_y + z\hat{e}_z$ is the position vector
 102 measured from the axis of rotation. Also l_c, u_c, p_c are constant dimensional characteristic values of
 103 length, filtration velocity, and pressure, respectively, used to convert the space variables, the
 104 filtration velocity, and the pressure into dimensionless forms. The gradient operator in equation (2)
 105 is defined in the form $\nabla \equiv [\hat{e}_x \partial(\)/\partial x + \hat{e}_y \partial(\)/\partial y + \hat{e}_z \partial(\)/\partial z]$.

106 The third term in the brackets in equation (2) represents the centrifugal force while the fourth term
 107 represents the Coriolis acceleration.

108 When fast transients or high frequency effects are of interest there is another extension to the
 109 Darcy equation that is applicable. Then, the time resolution obtained by assuming a very fast
 110 reaction of Darcy flow to changes and therefore the quasi-steady approximation which is inherent
 111 in the formulation of the Darcy law is not sufficient and a time derivative of the filtration velocity
 112 needs to be incorporated leading to the following dimensionless form of the extended Darcy
 113 equation in a rotating frame of reference

$$114 \quad \frac{Da Re M_f}{\phi} \rho \frac{\partial \mathbf{V}}{\partial t} + \mathbf{V} = -N_p \nabla p + Fr \rho \hat{e}_g - Cn \rho \hat{e}_\omega \times (\hat{e}_\omega \times \mathbf{X}) - \frac{\rho}{Ek_\Delta} \hat{e}_\omega \times \mathbf{V} \quad (4)$$

115 where the additional dimensionless groups that emerged are the Darcy number Da , and the
 116 Reynolds number Re

$$117 \quad Da = \frac{K_*}{l_c^2}, \quad Re = \frac{u_c l_c}{v_*} \quad (5)$$

118 and M_f is a ratio of heat capacities that its the definition will follow later. The corresponding
 119 length scale is a macro-level length scale, not the pore-size, despite the fact that it is the porous
 120 media filtration velocity that emerged in the definition of the Reynolds number. However the
 121 Reynolds number appears in equation (4) in a product combination with the Darcy number,
 122 bringing therefore the pore-scale effects into account too.

123 Following the definition of the dimensionless temperature in the form

$$124 \quad T = \frac{(T_* - T_o)}{\Delta T_c} \quad (6)$$

125 where T_* is the dimensional temperature, T_o is a reference value of temperature, and ΔT_c is a
 126 characteristic temperature difference, the dimensionless form of the energy equation subject to local
 127 thermal equilibrium (LTE or Lotheq) is presented in the form

$$128 \quad \frac{\partial T}{\partial t} + \mathbf{V} \cdot \nabla T = \frac{1}{Pe} \nabla^2 T \quad (7)$$

129 where Peclet number emerged as an additional dimensionless group, defined in the form

$$130 \quad Pe = \frac{u_c l_c}{\alpha_{e^*}} = Pr Re \quad (8)$$

131 where the porous media Prandtl number Pr is defined by

132 $Pr = \frac{V_*}{\alpha_{e^*}}$ (9)

133 The effective thermal diffusivity of the porous medium appearing in (8) and (9) is defined as
 134 $\tilde{\alpha}_{e^*} = k_{e^*}/\gamma_{e^*}$ and $M_f = \gamma_{f^*}/\gamma_{e^*}$ is the heat capacity ratio, i.e. the ratio between the effective heat
 135 capacity of the fluid phase and the effective heat capacity of the porous medium, where
 136 $\gamma_{e^*} = \gamma_{s^*} + \gamma_{f^*}$, $k_{e^*} = k_{s^*} + k_{f^*}$ are the effective heat capacity and effective thermal conductivity of the
 137 porous medium and subscripts "s" and "f" refer to the solid and fluid phases, respectively. Then
 138 the adjusted effective thermal diffusivity is defined as follows $\alpha_{e^*} = \tilde{\alpha}_{e^*}/M_f = k_{e^*}/\gamma_{f^*}$.

139 To complete the governing equations one needs a relationship between the density,
 140 temperature and pressure (and solute concentration when the fluid is a solution of soluble
 141 substances, e.g. salt in water, alcohol in water, etc., in which case an additional species equation
 142 needs to be added to). A linear approximation for this relationship is usually sufficiently accurate if
 143 the temperature and pressure differences are no excessively high. The dimensionless form of the
 144 linear approximation of the equation of state can be obtained by using the definition of the
 145 dimensionless temperature from equation (6) and the dimensionless pressure in the form
 146 $p = (p_* - p_o)/\Delta p_c$. Then the equation of state becomes

147 $\rho = [1 - \beta_r T + \beta_p p]$ (10)

148 where $\rho = \rho_*/\rho_o$ is the dimensionless density, and $\beta_r = \beta_{T^*} \Delta T_c$, $\beta_p = \beta_{p^*} \Delta p_c$ are the
 149 dimensionless thermal expansion and pressure compression coefficients, respectively. For most
 150 fluid flows and especially for incompressible flows, i.e. flows of liquids, $\beta_p \ll \beta_r$. Therefore the
 151 common approximation of the dimensionless equation of state is

152 $\rho = [1 - \beta_r T]$ (11)

153 There are some identities relevant to flows in a rotating frame of reference and in buoyancy flows
 154 that are useful in the following derivations. These identities are

155 $\hat{e}_g = \nabla(\hat{e}_g \cdot X)$ (12)

156 $\hat{e}_\omega \times (\hat{e}_\omega \times X) = -\nabla \left[\frac{1}{2} (\hat{e}_\omega \times X) \cdot (\hat{e}_\omega \times X) \right]$ (13)

157 $\hat{e}_\omega \times (\hat{e}_\omega \times X) = (\hat{e}_\omega \cdot X) \hat{e}_\omega - X$ (14)

158 Their proof can be found in Vadasz [3].

159 Although for a significantly high number of practical instances Darcy's model (or its extension)
 160 for a rotating frame of reference is sufficient for representing the effects of rotation, non-Darcy
 161 models have been used as well. Their relevance and limitations are subject to professional discourse
 162 (e.g. Nield [68, 69, 70] and Vafai and Kim [71]).

163

164 3. Taylor-Proudman Columns and Geostrophic Flow in Rotating Porous Media

165 By using equations (12) and (13), considering isothermal conditions (no heat transfer) and
 166 consequently the density is constant $\rho_* = \rho_o$ hence $\rho = 1$, Darcy equation (2) becomes

167
$$V = -\nabla \left[N_p p - Fr (\hat{e}_g \cdot X) - Cn \left(\frac{1}{2} (\hat{e}_\omega \times X) \cdot (\hat{e}_\omega \times X) \right) \right] - \frac{1}{Ek_\Delta} \hat{e}_\omega \times V$$
 (15)

168 The term under the common gradient operator is a reduced pressure p_r , defined as

169
$$p_r = N_p p - Fr (\hat{e}_g \cdot X) - \frac{Cn}{2} (\hat{e}_\omega \times X) \cdot (\hat{e}_\omega \times X)$$
 (16)

170 By using (16) and choosing the direction of the angular velocity of rotation to be aligned with the
 171 vertical axis, i.e. $\hat{e}_\omega = \hat{e}_z$, the Darcy equation (2) can be presented in the following rearranged form
 172
$$[Ek_\Delta + \hat{e}_z \times] V = -\nabla (Ek_\Delta p_r)$$
 (17)

173 For typical values of viscosity, porosity and permeability the range of variation of Ekman number
 174 can be evaluated in some engineering applications. Consequently, the angular velocity may vary
 175 from 10 rpm to 10,000 rpm leading to Ekman numbers in the range from $Ek_A = 1$ to $Ek_A = 10^{-3}$.
 176 The latter value is very small, pertaining to the conditions considered here. Therefore, in the limit of
 177 $Ek_A \rightarrow 0$, say $Ek_A = 0$, equation (17) takes the simplified form

178 $\hat{\mathbf{e}}_z \times \mathbf{V} = -\nabla(Ek_A p_R)$ (18)

179 and the effect of permeability variations disappears. Taking the "curl" of equation (18) leads to
 180 $\nabla \times (\hat{\mathbf{e}}_z \times \mathbf{V}) = 0$ (19)

181 Evaluating the "curl" operator on the cross product of the left-hand side of equation (19) leads to
 182 $(\hat{\mathbf{e}}_z \cdot \nabla) \mathbf{V} = 0$ (20)

183 Equation (20) is identical to the Taylor-Proudman theorem for pure fluids (non-porous domains); it
 184 thus represents the proof of the Taylor-Proudman theorem in porous media, and can be presented
 185 in the following simplified form

186 $\frac{\partial \mathbf{V}}{\partial z} = 0$ (21)

187 The conclusion expressed by equation (21) is that $\mathbf{V} = \mathbf{V}(x, y)$, i.e. it cannot be a function of z ,
 188 where z is the direction of the angular velocity vector. This means that all filtration velocity
 189 components can vary only in the plane perpendicular to the angular velocity vector. This result
 190 leads to the existence of Taylor-Proudman columns in rotating porous media as presented in detail
 191 by Vadasz [3]. The consequence of this result can be demonstrated by considering a particular
 192 example that was presented by Vadasz [36] (see Greenspan [72] for the corresponding example in
 193 pure fluids).

194 A further significant consequence of equation (21) is represented by a geostrophic type of flow.
 195 Taking the z -component of equation (21) yields $\partial w / \partial z = 0$, and the continuity equation (1)
 196 becomes two dimensional

197 $\frac{\partial u}{\partial x} + \frac{\partial v}{\partial y} = 0$ (22)

198 Therefore the flow at high rotation rates has a tendency towards two-dimensionality and a stream
 199 function, ψ , can be introduced for the flow in the $x - y$ plane in the form

200 $u = -\frac{\partial \psi}{\partial y}; \quad v = \frac{\partial \psi}{\partial x}$ (23)

201 which satisfies identically the continuity equation (1). Substituting u and v with their stream
 202 function representation given by equation (23) into equation (18) yields

203 $\frac{\partial \psi}{\partial x} = \frac{\partial(Ek_A p_R)}{\partial x}$ (24)

204 $\frac{\partial \psi}{\partial y} = \frac{\partial(Ek_A p_R)}{\partial y}$ (25)

205 As both the pressure and the stream function can be related to an arbitrary reference value, the
 206 conclusion from equations (24) and (25) is that the stream function and the pressure are the same in
 207 the limit of high rotation rates ($Ek \rightarrow 0$). This type of geostrophic flow means that isobars represent
 208 streamlines at the leading order, for $Ek \rightarrow 0$.
 209

210 4. Natural Convection due to Centrifugal Buoyancy

211 Natural convection is the effect of flow and convection heat transfer due to the existence of
 212 density gradients in a body force field (such as gravity or centrifugal force field). As density
 213 depends on temperature as demonstrated in the derivation of the equation of state, temperature

214 gradients may create natural convective flows when a body force field is present. What
 215 characterizes natural convection is the lack of a known value of characteristic filtration velocity that
 216 can be applied upfront in a problem. No characteristic velocity can be specified because the latter is
 217 dictated by the temperature gradients and their resulting buoyancy rather than being known
 218 upfront. Therefore a sensible choice of u_c would be $u_c = \alpha_{e^*}/l_c$. With this choice of u_c the
 219 Froude number Fr , the pressure number N_p , and the centrifugal dimensionless group Cn in
 220 equations (12) and (14) become $Fr = g_* K_* l_c / v_* \alpha_{e^*}$, $N_p = K_* \Delta p_c / \mu_* \alpha_{e^*}$, $Cn = \omega_*^2 l_c^2 K_* / v_* \alpha_{e^*}$. Without
 221 loss of generality for the same reason as for the filtration velocity one can chose the characteristic
 222 pressure difference to be such that the pressure number N_p becomes unity, i.e. $\Delta p_c = \mu_* \alpha_{e^*} / K_*$
 223 leading to $N_p = 1$. Also the Reynolds number in equation (5) renders into the reciprocal Prandtl
 224 number $Re = \alpha_{e^*} / v_* = 1/Pr$ and the Peclet number in equations (7) and (8) becomes equal to one by
 225 definition $Pe = u_c l_c / \alpha_{e^*} = \alpha_{e^*} l_c / l_c \alpha_{e^*} = 1$. One may define the effective Prandtl number in terms of
 226 the effective thermal diffusivity $\tilde{\alpha}_{e^*}$ (see the equation and the text following equation (9))
 227 $Pr_e = v_* / \tilde{\alpha}_{e^*} = Pr / M_f$. Then the coefficient to the time derivative term in equation (4) becomes
 228 $DaReM_f / \phi = DaM_f / \phi Pr = Da / \phi Pr_e = 1/Va$ a new dimensionless group that Straughan [73] named
 229 the Vadasz number (Va), or the Vadasz coefficient named by Straughan [73] (see also Sheu [74] and
 230 Govender [26]). By using equations (11), (12) and (13) leads to transforming equations (2) and (4)
 231 into the following form

$$232 \quad \mathbf{V} = -\nabla p_r + Ra_g T \hat{\mathbf{e}}_g - Ra_\omega T [(\hat{\mathbf{e}}_\omega \cdot \mathbf{X}) \hat{\mathbf{e}}_\omega - \mathbf{X}] - \frac{1}{Ek_\Delta} \hat{\mathbf{e}}_\omega \times \mathbf{V} \quad (26)$$

$$233 \quad \frac{1}{V_a} \frac{\partial \mathbf{V}}{\partial t} + \mathbf{V} = -\nabla p_r + Ra_g T \hat{\mathbf{e}}_g - Ra_\omega T [(\hat{\mathbf{e}}_\omega \cdot \mathbf{X}) \hat{\mathbf{e}}_\omega - \mathbf{X}] - \frac{1}{Ek_\Delta} \hat{\mathbf{e}}_\omega \times \mathbf{V} \quad (27)$$

234 The product of β_T by Fr and Cn produced two new dimensionless groups in the form of the
 235 gravity related Rayleigh number and the centrifugal Rayleigh number, respectively in the form

$$236 \quad Ra_g = Fr \beta_T = \frac{\beta_T \Delta T_c g_* K_* l_c}{V_* \alpha_{e^*}} \quad (28)$$

$$237 \quad Ra_\omega = Cn \beta_T = \frac{\beta_T \Delta T_c \omega_*^2 l_c^2 K_*}{V_* \alpha_{e^*}} \quad (29)$$

238 The particular cases when $\hat{\mathbf{e}}_g = -\hat{\mathbf{e}}_z$ and $\hat{\mathbf{e}}_\omega = \hat{\mathbf{e}}_z$ will be considered later. Subject to this orientation
 239 of the gravity and angular velocity of rotation equations (26) and (27) take the form

$$240 \quad \mathbf{V} = -\nabla p_r + Ra_g T \hat{\mathbf{e}}_z - Ra_\omega T (x \hat{\mathbf{e}}_x + y \hat{\mathbf{e}}_y) - \frac{1}{Ek_\Delta} \hat{\mathbf{e}}_z \times \mathbf{V} \quad (30)$$

$$241 \quad \frac{1}{V_a} \frac{\partial \mathbf{V}}{\partial t} + \mathbf{V} = -\nabla p_r + Ra_g T \hat{\mathbf{e}}_z - Ra_\omega T (x \hat{\mathbf{e}}_x + y \hat{\mathbf{e}}_y) - \frac{1}{Ek_\Delta} \hat{\mathbf{e}}_z \times \mathbf{V} \quad (31)$$

242 The vector $\mathbf{r} = (x \hat{\mathbf{e}}_x + y \hat{\mathbf{e}}_y)$ in equations (30) and (31) represents the perpendicular radius vector
 243 from the axis of rotation to any point in the flow domain.

244 Three dimensionless groups emerged in equation (30) when fast transients or high frequencies are
 245 not of interest. These dimensionless groups control the significance of the different phenomena.
 246 Therefore, the value of Ekman number (Ek_Δ) controls the significance of the Coriolis effect, and the
 247 ratio between the gravity related Rayleigh number (Ra_g) and centrifugal Rayleigh number (Ra_ω)
 248 controls the significance of gravity with respect to centrifugal forces as far as natural convection is
 249 concerned. This ratio is $Ra_g / Ra_\omega = g_* / \omega_*^2 l_c$. When fast transients or high frequencies are of interest
 250 equation (27) is to be considered. In such a case one additional dimensionless group emerged, the
 251 Va number representing the ratio between two characteristic frequencies, i.e. the fluid flow
 252 frequency $\omega_{v*} = \phi v_* / K_*$ and the thermal diffusion frequency $\omega_{\alpha*} = \tilde{\alpha}_{e^*} / l_c^2$, i.e.

253 $Va = \omega_{v*}/\omega_{\alpha*} = \phi v_* l_c^2 / K_* \tilde{\alpha}_{\epsilon*} = \phi Pr_e / Da$, or alternatively the ratio between two time scales, i.e. the
 254 thermal diffusion time scale $\tau_{\alpha*} = l_c^2 / \tilde{\alpha}_{\epsilon*}$, and the fluid flow time scale $\tau_{v*} = K_* / \phi v_*$, i.e.
 255 $Va = \tau_{\alpha*} / \tau_{v*} = \phi v_* l_c^2 / K_* \tilde{\alpha}_{\epsilon*} = \phi Pr_e / Da$. In addition to such cases equation (27) should be used also
 256 when the effective Prandtl number is of the order of magnitude of Darcy number, i.e. $Pr_e = O(Da)$
 257 i.e. a very small number (as $Da \ll 1$ in most porous media). Such small values of the Prandtl
 258 number are typical for liquid metals. In such cases too the time derivative term in equation (27)
 259 should be retained.

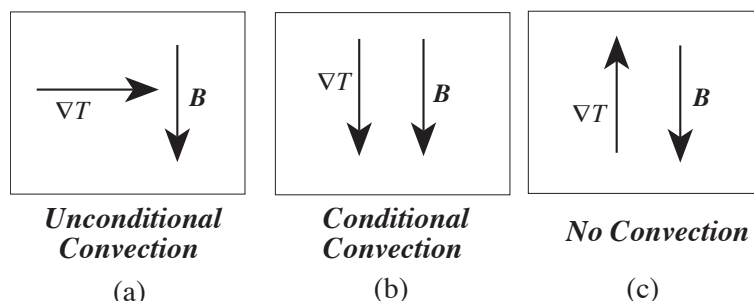
260 Considering the Darcy regime subject to a centrifugal body force and by neglecting gravity
 261 effects ($Ra_g / Ra_\omega \ll 1$) equations (1), (7) and (26) with $Ra_g = 0$ and $Pe = 1$ represent the
 262 mathematical model for this case. The objective in the first instance is to establish the convective
 263 flow under small rotation rates, then $Ek \gg 1$, and as a first approximation the Coriolis effect can
 264 be neglected, i.e., $Ek \rightarrow \infty$. Following these conditions the governing equations become (by using
 265 identity (14))

$$266 \nabla \cdot V = 0 \quad (32)$$

$$267 V = -[\nabla p - Ra_\omega T \hat{e}_\omega \times (\hat{e}_\omega \times X)] \quad (33)$$

$$268 \frac{\partial T}{\partial t} + V \cdot \nabla T = \nabla^2 T \quad (34)$$

269 There are three cases corresponding to the relative orientation of the temperature gradient with
 270 respect to the centrifugal body force as presented in Figure 1. Case 1(a) in Figure 1 corresponds to a
 271 temperature gradient, which is perpendicular to the direction of the centrifugal body force and
 272 leads to unconditional convection. The solution representing this convection pattern is presented by
 273 Vadasz [34, 3, 4]. Cases 1(b) and 1(c) in Figure 1 corresponding to temperature gradients collinear
 274 with the centrifugal body force represent stability problems and hence our present focus. The
 275 objective is then to establish the stability condition as well as the convection pattern when this
 276 stability condition is not satisfied.



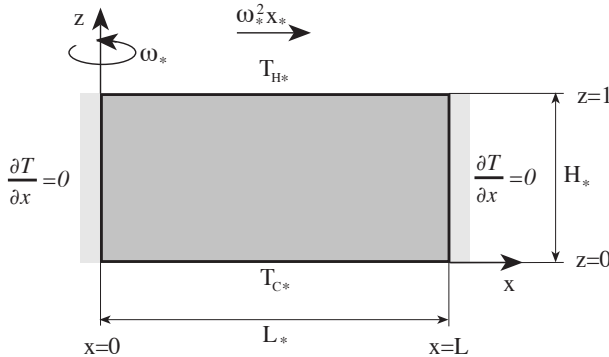
277 (a) (b) (c)

278 **Figure 1.** The effect of the relative orientation of the temperature gradient with respect to the body
 279 force on the setup of convection.

281 An example of a case when the imposed temperature is perpendicular to the centrifugal body force
 282 is a rectangular porous domain rotating about the vertical axis, heated from above and cooled from
 283 below. For this case the centrifugal buoyancy term in equation (33) becomes $Ra_\omega T x \hat{e}_x$ leading to
 284
 285 $V = -\nabla p - Ra_\omega T x \hat{e}_x$ (35)

286 An analytical two-dimensional solution to this problem (see Figure 2) for a small aspect ratio of the
 287 domain was presented by Vadasz [34, 3, 4]. The solution to the non-linear set of partial differential
 288 equations was obtained through an asymptotic expansion of the dependent variables in terms of a
 289 small parameter representing the aspect ratio of the domain.

290 The convection in the core region far from the sidewalls was the objective of the investigation. To
 291 first order accuracy, the heat transfer coefficient represented by the Nusselt number was evaluated
 292 in the form



293

294

Figure 2: A rotating rectangular porous domain heated from above, cooled from below, and insulated on its sidewalls. (courtesy Elsevier Science Ltd.)

295

296

$$297 \quad Nu = - \left[1 + \frac{Ra_{\omega}}{24} + O(H^2) \right] \quad (36)$$

298

where Nu is the Nusselt number and the length scale used in the definition of Ra_{ω} , equation (54), was $l_c = H_*$. Vadasz [37] used a different approach to solve a similar problem without the restriction of a small aspect ratio. A direct extraction and substitution of the dependent variables was found to be useful for de-coupling the non-linear partial differential equations, resulting in a set of independent non-linear ordinary differential equations, which was solved analytically. To obtain an analytical solution to the non-linear convection problem we assume that the vertical component of the filtration velocity, w , and the temperature T are independent of x , i.e., $\partial w / \partial x = \partial T / \partial x = 0 \quad \forall x \in (0, L)$, being functions of z only. It is this assumption that will subsequently restrict the validity domain of the results to moderate values of Ra_{ω} (practically $Ra_{\omega} < 5$). Subject to the assumptions of two-dimensional flow $v = 0$ and $\partial(\cdot) / \partial y = 0$ and that w and T are independent of x the governing equations take the form

$$309 \quad \frac{\partial u}{\partial x} + \frac{dw}{dz} = 0 \quad (37)$$

$$310 \quad u = - \frac{\partial p}{\partial x} - Ra_{\omega} x T \quad (38)$$

$$311 \quad w = - \frac{\partial p}{\partial z} \quad (39)$$

$$312 \quad \frac{d^2 T}{dz^2} - w \frac{dT}{dz} = 0 \quad (40)$$

313 The method of solution consists of extracting T from equation (38) and expressing it explicitly in
 314 terms of $u, \partial p / \partial x$ and x . This expression of T is then introduced into equation (40) and the
 315 derivative $\partial / \partial x$ is applied to the result. Then, substituting the continuity equation (37) in the form
 316 $\partial u / \partial x = -dw / dz$ and equation (39) into the results yields a non-linear ordinary differential
 317 equation for w in the form

$$318 \quad \frac{d^3 w}{dz^3} - w \frac{d^2 w}{dz^2} = 0 \quad (41)$$

319

320

321

322

323

324

An interesting observation regarding equation (41) is the fact that it is identical to the Blasius equation for boundary layer flows of pure fluids (non-porous domains) over a flat plate. To observe this, one simply has to substitute $w(z) = -f(z)/2$ to obtain $2f'' + ff'' = 0$, which is the Blasius equation. Unfortunately, no further analogy to the boundary layer flow in pure fluids exists, predominantly due to the different boundary conditions and because the derivatives $[d(\cdot) / dz]$ and the flow (w) are in the same direction. The solutions for the temperature T and the horizontal

325 component of the filtration velocity u , are related to the solution of the ordinary differential
326 equation

327 $\varphi' \varphi''' - \varphi''^2 + \varphi \varphi'^2 = 0$ (42)

328 where $(\cdot)'$ stands for $d(\cdot)/dz$ and

329 $u = x \varphi(z)$ (43)

330 $T(z) = -\frac{1}{Ra_\omega} [P + \varphi(z)]$ (44)

331 where P is a constant defined by

332 $P = -Ra_\omega \int_0^1 T(z) dz$ (45)

333 The relationship (45) is a result of imposing a condition of no net flow through any vertical
334 cross-section in the domain, stating that $\int_0^1 u dz = 0$.

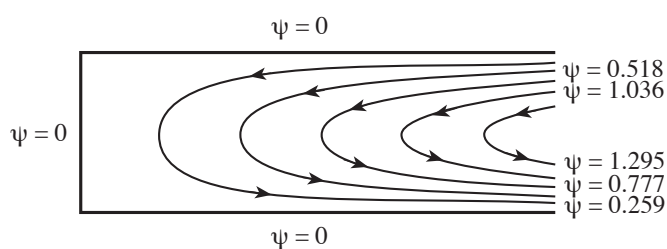
335 The following boundary conditions are required to the solution of (41) for w :
336 $w = 0$ at $z = 0$ and $z = 1$ representing the impermeability condition at the solid boundaries and
337 $T = 0$ at $z = 0$ and $T = 1$ at $z = 1$. Since $\partial u / \partial x = \varphi$ according to equation (43), then following the
338 continuity equation (37) $\varphi = -dw/dz$ and the temperature boundary conditions can be converted
339 into conditions in terms of w by using equation (44), leading to the following complete set of
340 boundary conditions for w :

341 $z = 0 : w = 0 \quad \text{and} \quad \frac{dw}{dz} = P$ (46)

342 $z = 1 : w = 0 \quad \text{and} \quad \frac{dw}{dz} = P + Ra_\omega$ (47)

343 Equations (46) and (47) represent four boundary conditions, while only three are necessary to solve
344 the third order equation (41). The reason for the fourth condition comes from the introduction of the
345 constant P , whose value remains to be determined. Hence, the additional two boundary
346 conditions are expressed in terms of the unknown constant P and the solution subject to these
347 four conditions will determine the value of P as well. A method similar to Blasius's method of
348 solution was applied to solve equation (41). Therefore, $w(z)$ was expressed as a finite power series
349 and the objective of the solution was to determine the power series coefficients. Once the solution
350 for $w(z)$ and the value of P were obtained, u and T were evaluated by using
351 $\varphi(z) = -dw/dz$ and equations (43) and (44).

352



353

354 **Figure 3:** Graphical description of the resulting flow field; five streamlines equally spaced between their
355 minimum value $\psi_{\min} = 0$ at the rigid boundaries and their maximum value $\psi_{\max} = 1.554$. The values in the
356 figure correspond to every other streamline. (courtesy Elsevier Science Ltd.)

357

358 For presentation purposes a stream function ψ was introduced to plot the results ($u = \partial\psi/\partial z$, $w = -\partial\psi/\partial x$). An example of the flow field represented by the streamlines is
359 presented in Figure 9 for $Ra_\omega = 4$ and for an aspect ratio of 3 (excluding a narrow region next to
360 the sidewall at $x = L$). Outside this narrow region next to $x = L$ the streamlines remain open on
361 the right hand side. They are expected to close in the end region. On the left-hand side, however,
362 the streamlines close throughout the domain. The reason for this, is the centrifugal acceleration,
363

which causes u to vary linearly with x , thus creating (due to the continuity equation) a non-vanishing vertical component of the filtration velocity w at all values of x . The local Nusselt number Nu , representing the local vertical heat flux was evaluated as well by using the definition $Nu = -\partial T / \partial z|_{z=0}$ and using the solution for T . A comparison between the heat flux results obtained from this solution and the results obtained by Vadasz [34] using an asymptotic method was presented graphically by Vadasz [37]. The two results compare well as long as Ra_ω is very small. However, for increasing values of Ra_ω the deviation from the linear relationship pertaining to the first order asymptotic solution ($Nu = 1 + Ra_\omega / 24$, according to Vadasz [34]) was evident. The stability of this convection flow was not evaluated, although it is of extreme interest. This would be an interesting though not simple task recommended for future research.

The problem of stability of free convection in a rotating porous layer when the temperature gradient is collinear with the centrifugal body force was treated by Vadasz [38] and Vadasz [40] for a narrow layer adjacent to the axis of rotation (Vadasz [38]) and distant from the axis of rotation (Vadasz [40]), respectively. The problem formulation corresponding to the latter case is presented in Figure 4. In order to include explicitly the dimensionless offset distance from the axis of rotation x_0 , and to keep the coordinate system linked to the porous layer, equation (33) was presented in the form

$$V = -\nabla p - [Ra_{\omega\omega} + Ra_\omega x] T \hat{e}_x \quad (48)$$

Two centrifugal Rayleigh numbers appear in equation (48); the first one, representing the contribution of the offset distance from the rotation axis to the centrifugal buoyancy is $Ra_{\omega\omega} = \beta_{T^*} \Delta T_c \omega_*^2 x_{0*} L_* K_o / \alpha_{e^*} v_*$, while the second, $Ra_\omega = \beta_{T^*} \Delta T_c \omega_*^2 L_*^2 K_o / \alpha_{e^*} v_*$, represents the contribution of the horizontal location within the porous layer to the centrifugal buoyancy. The ratio between the two centrifugal Rayleigh numbers is dimensionless reciprocal distance from the axis of rotation

$$\eta = \frac{Ra_\omega}{Ra_{\omega\omega}} = \frac{1}{x_0} \quad (49)$$

and can be introduced as a parameter in the equations transforming equation (48) into the form

$$V = -\nabla p - Ra_{\omega\omega} [1 + \eta x] T \hat{e}_x \quad (50)$$

From equation (50) it is observed that when the porous layer is far away from the axis of rotation then $\eta \ll 1$ ($x_0 \gg 1$) and the contribution of the term ηx is not significant, while for a layer close enough to the rotation axis $\eta \gg 1$ ($x_0 \ll 1$) and the contribution of the first term becomes insignificant. In the first case the only controlling parameter is $Ra_{\omega\omega}$ while in the latter case the only controlling parameter is $Ra_\omega = \eta Ra_{\omega\omega}$. The flow boundary conditions are $V \cdot \hat{e}_n = 0$ on the boundaries, where \hat{e}_n is a unit vector normal to the boundary. These conditions stipulate that all boundaries are rigid and therefore non-permeable to fluid flow. The thermal boundary conditions are: $T = 0$ at $x = 0$, $T = 1$ at $x = 1$ and $\nabla T \cdot \hat{e}_n = 0$ on all other walls representing the insulation condition on these walls.

The governing equations accept a basic motionless conduction solution in the form

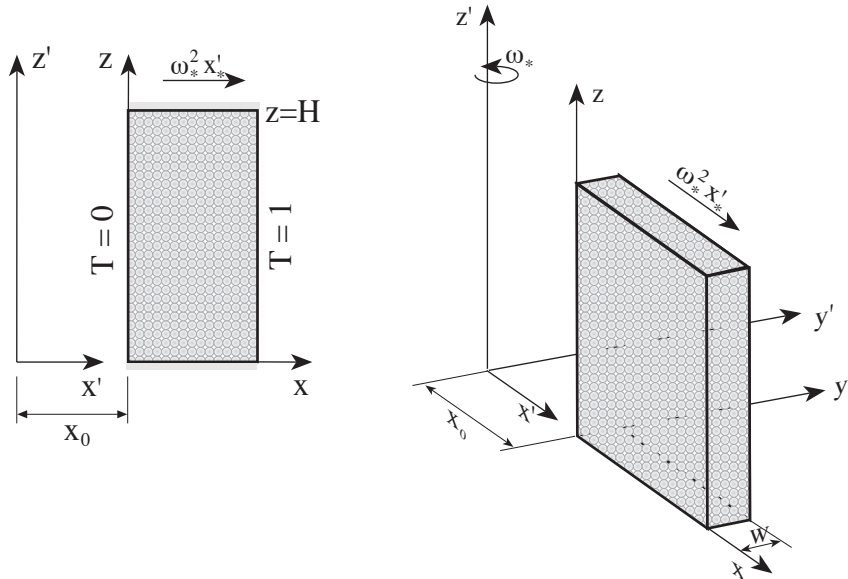
$$[V_b, T_b, p_b] = [0, x, (-Ra_{\omega\omega} (x^2/2 + \eta x^3/3) + C)] \quad (51)$$

The objective of the investigation was to establish the condition when the motionless solution (51) is not stable and consequently a resulting convection pattern appears. Therefore a linear stability analysis was employed, representing the solution as a sum of the basic solution (51) and small perturbations in the form

$$[V, T, p] = [V_b + V', T_b + T', p_b + p'] \quad (52)$$

where $(\cdot)'$ stands for perturbed values. Solving the resulting linearized system for the perturbations by assuming a normal modes expansion in the y and z directions, and $\theta(x)$ in

409 the x direction, i.e., $T' = A_x \theta(x) \exp[\sigma t + i(\kappa_y y + \kappa_z z)]$, and using the Galerkin method to solve for
 410 $\theta(x)$ one obtains at marginal stability, i.e., for $\sigma = 0$, a homogeneous set of linear algebraic
 411 equations. This homogeneous linear system accepts a non-zero solution only for particular values of
 412 $Ra_{\omega\omega}$ such that its determinant vanishes. The solution of this system was evaluated up to order 7
 413 for different values of η , representing the offset distance from the axis of rotation.
 414



415
 416 **Figure 4:** A rotating fluid saturated porous layer distant from the axis of rotation and subject to different
 417 temperatures at the sidewalls.

418
 419 However, useful information was obtained by considering the approximation at order 2. At this
 420 order the system reduces to two equations, which lead to the characteristic values of $Ra_{\omega\omega}$ in the
 421 form

$$422 R_{o,c} = \frac{\beta[(1+\alpha)^2 + (4+\alpha)^2]}{2\alpha(\beta^2 - \gamma^2)} \pm \frac{\sqrt{\beta^2[(1+\alpha)^2 + (4+\alpha)^2]^2 - 4(\beta^2 - \gamma^2)(1+\alpha)^2(4+\alpha)^2}}{2\alpha(\beta^2 - \gamma^2)} \quad (53)$$

423 where the following notation was used

$$424 R_o = \frac{Ra_{\omega\omega}}{\pi^2}; \quad R = \frac{Ra_{\omega}}{\pi^2}; \quad \alpha = \frac{\kappa^2}{\pi^2}; \quad \beta = 1 + \frac{\eta}{2}; \quad \gamma^2 = \frac{256\eta^2}{81\pi^4} \quad (54)$$

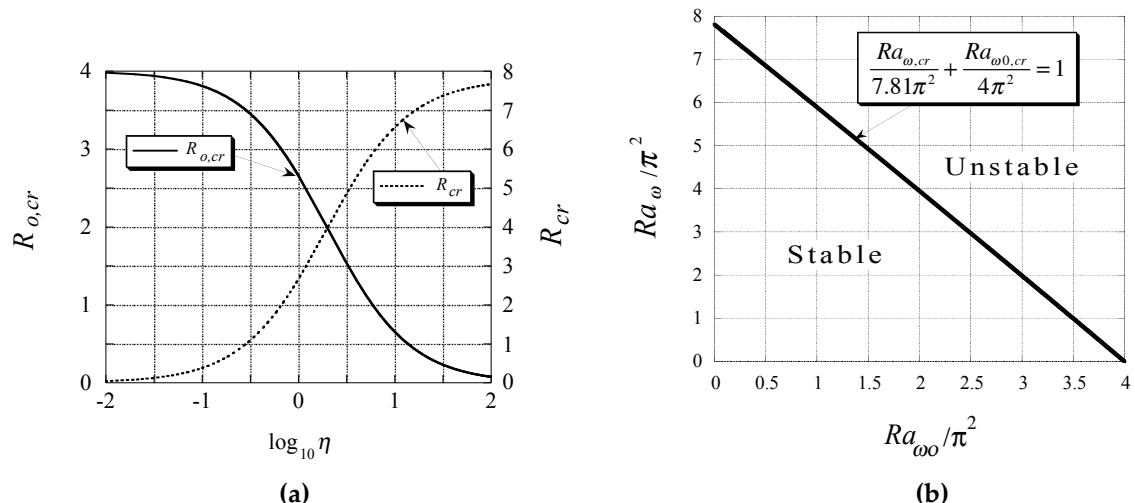
425 and κ is the wavenumber such that $\kappa^2 = \kappa_y^2 + \kappa_z^2$ while the subscript c in equation (53)
 426 represents characteristic (neutral) values (values for which $\sigma = 0$). A singularity in the solution for
 427 $R_{o,c}$, corresponding to the existence of a single root for $R_{o,c}$, appears when $\beta^2 = \gamma^2$. This
 428 singularity persists at higher orders as well. Resolving for the value of η when this singularity
 429 occurs shows that it corresponds to negative η values implying that the location of the rotation
 430 axis falls within the boundaries of the porous domain (or to the right side of the hot wall - a case of
 431 little interest due to its inherent unconditional stability). This particular case will be discussed later
 432 in this section. The critical values of the centrifugal Rayleigh number as obtained from the solution
 433 up to order 7 are presented graphically in Figure 5(a) in terms of both $R_{o,cr}$ and R_{cr} as a function
 434 of the offset parameter η . The results presented in Figure 5 are particularly useful in order to
 435 indicate the stability criterion for all positive values of η . It can be observed from the figure that as
 436 the value of η becomes small, i.e. for a porous layer far away from the axis of rotation, the critical
 437 centrifugal Rayleigh number approaches a limit value of $4\pi^2$. This corresponds to the critical
 438 Rayleigh number in a porous layer subject to gravity and heated from below. For high values of η

439 it is appropriate to use the other centrifugal Rayleigh number R , instead of R_o , by introducing the
 440 relationship $R = \eta R_o$ (see equations (49) and (54)) in order to establish and present the stability
 441 criterion. It is observed from Fig. 5(a) that as the value of η becomes large, i.e. for a porous layer
 442 close to the axis of rotation, the critical centrifugal Rayleigh number approaches a limit value of
 443 $7.81\pi^2$. This corresponds to the critical Rayleigh number for the problem of a rotating layer
 444 adjacent to the axis of rotation as presented by Vadasz [38]. The stability map on the $Ra_o - Ra_{\omega o}$
 445 plane is presented in Figure 5(b), showing that the plane is divided between the stable and unstable
 446 zones by the straight line $(Ra_{\omega,cr}/7.81\pi^2) + (Ra_{\omega 0,cr}/4\pi^2) = 1$.

447 The results for the convective flow field are presented graphically in Figure 6 following Vadasz
 448 [40], where it was concluded that the effect of the variation of the centrifugal acceleration within the
 449 porous layer is definitely felt when the box is close to the axis of rotation, corresponding to an
 450 eccentric shift of the convection cells towards the sidewall at $x = 1$. However, when the layer is
 451 located far away from the axis of rotation (e.g. $x_0 = 50$) the convection cells are concentric and
 452 symmetric with respect to $x = 1/2$ as expected for a porous layer subject to gravity and heated
 453 from below (here "below" means the location where $x = 1$).

454 Although the linear stability analysis is sufficient for obtaining the stability condition of the
 455 motionless solution and the corresponding eigenfunctions describing qualitatively the convective
 456 flow, it cannot provide information regarding the values of the convection amplitudes, nor
 457 regarding the average rate of heat transfer. To obtain this additional information, Vadasz and Olek
 458 [46] analyzed and provided a solution to the non-linear equations by using Adomian's
 459 decomposition method to solve a system of ordinary differential equations for the evolution of the
 460 amplitudes.

461



462

463

464 **Figure 5: (a)** The variation of the critical values of the centrifugal Rayleigh numbers as a function of η ;
 465 **(b)** The stability map on the $Ra_o - Ra_{\omega o}$ plane showing the division of the plane.

466

467 This system of equations was obtained by using the first three relevant Galerkin modes for the
 468 stream function and the temperature in the form

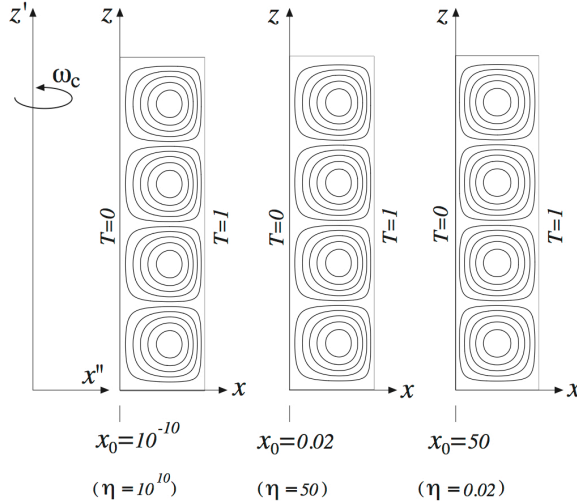
$$469 \quad \psi = 2\theta\sqrt{2\bar{\gamma}(R-1)}X(t)\sin(\pi x)\sin\left(\frac{\pi z}{H}\right) \quad (55)$$

$$470 \quad T = x + \frac{2\sqrt{2\bar{\gamma}(R-1)}}{\pi R}Y(t)\sin(\pi x)\cos\left(\frac{\pi z}{H}\right) + \frac{(R-1)}{\pi R}Z(t)\sin(2\pi x) \quad (56)$$

471 where $\bar{\gamma} = H^2/(H^2 + 1)$, $\theta = (H^2 + 1)/H$, H being the layer's aspect ratio, $R = \xi/\pi^2\theta^2$,
 472 $\xi = Ra_{\omega o} + Ra_o/2$, and X, Y, Z the possibly time dependent amplitudes of convection. In this

473 model it was considered of interest including the time derivative term in Darcy's equation in the
 474 form $(1/Va)\partial V/\partial t$, where $Va = \phi Pr_e/Da$, and Da, Pr_e are the Darcy and the effective Prandtl
 475 numbers, respectively, defined as $Da = K_*/L_*^2$ and $Pr_e = v_*/\tilde{\alpha}_{e*}$ (see equation (58) with $Ra_g = 0$
 476 and $Ek \rightarrow \infty$). The reason for including the time derivative term in the Darcy equation was the fact
 477 that one anticipates oscillatory and possibly chaotic solutions for which very high frequencies may
 478 occur. Then, the following equations were obtained for the time evolution of the amplitudes
 479 $X(t), Y(t), Z(t)$

480



481

482 **Figure 6:** The convective flow field at marginal stability for three different values of x_0 ; 10 stream lines
 483 equally divided between ψ_{\min} and ψ_{\max} . At $x_0 = 10^{-10}$: $\psi_{\min} = -1.378$; $\psi_{\max} = 1.378$, at $x_0 = 0.02$: $\psi_{\min} = -1.374$;
 484 $\psi_{\max} = 1.374$ and at $x_0 = 50$: $\psi_{\min} = -1.319$; $\psi_{\max} = 1.319$.

485

$$486 \dot{X} = \alpha(Y - X) \quad (57)$$

$$487 \dot{Y} = RX - Y - (R - 1)XZ \quad (58)$$

$$488 \dot{Z} = 4\bar{\gamma}(XY - Z) \quad (59)$$

489 where $\alpha = \bar{\gamma}Va/\pi^2$, and R is a rescaled Rayleigh number introduced above according to the
 490 definitions in the text following equation (56). The results obtained are presented in Figure 7 in the
 491 form of projection of trajectories data points onto the $Y - X$ and $Z - X$ planes. Different
 492 transitions as the value of R varies are presented and they relate to the convective fixed point
 493 which is a stable simple node in Figure 7(a), a stable spiral in Figures 7(b) and 7(c), and loses
 494 stability via an inverse Hopf bifurcation in Figure 7(d), where the trajectory describes a limit cycle,
 495 moving towards a chaotic solution presented in Figures 7(e) and (f). A further transition from chaos
 496 to a periodic solution was obtained at a value of R slightly above 100, which persists over a wide
 497 range of R values. This periodic solution is presented in Figures 7(g) and 7(h) for $R = 250$.

498 Previously in this section (see equation (53)) a singularity in the solution was identified and
 499 associated with negative values of the offset distance from the axis of rotation. It is this resulting
 500 singularity and its consequences, which were investigated by Vadasz [41] and are the objective of
 501 the following presentation. As this occurs at negative values of the offset distance from the axis of
 502 rotation it implies that the location of the rotation axis falls within the boundaries of the porous
 503 domain, as presented in Fig. 8. This particular axis location causes positive values of the centrifugal
 504 acceleration on the right side of the rotation axis and negative values on its left side. The rotation
 505 axis location implies that the value of x_0 is not positive.

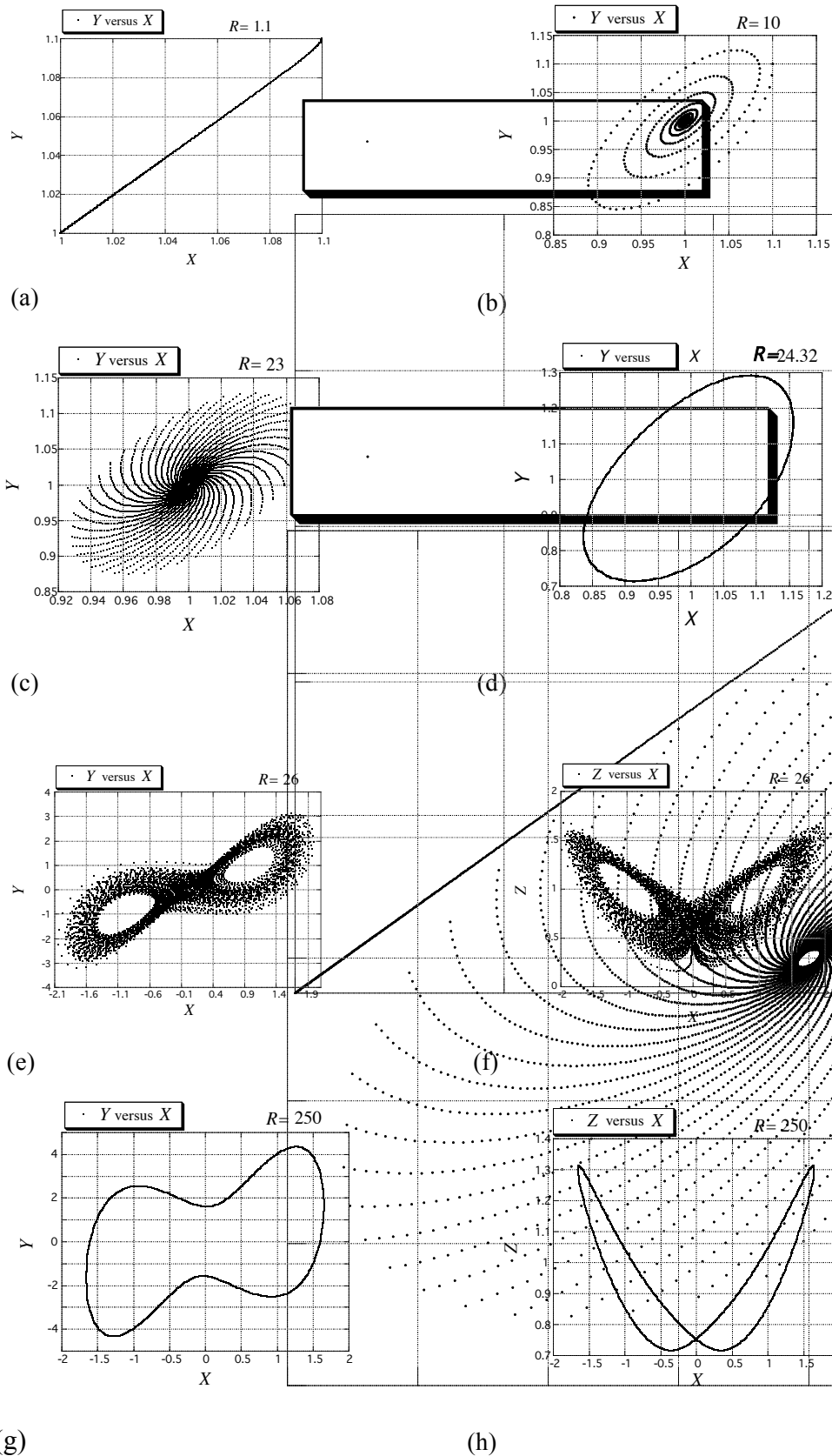
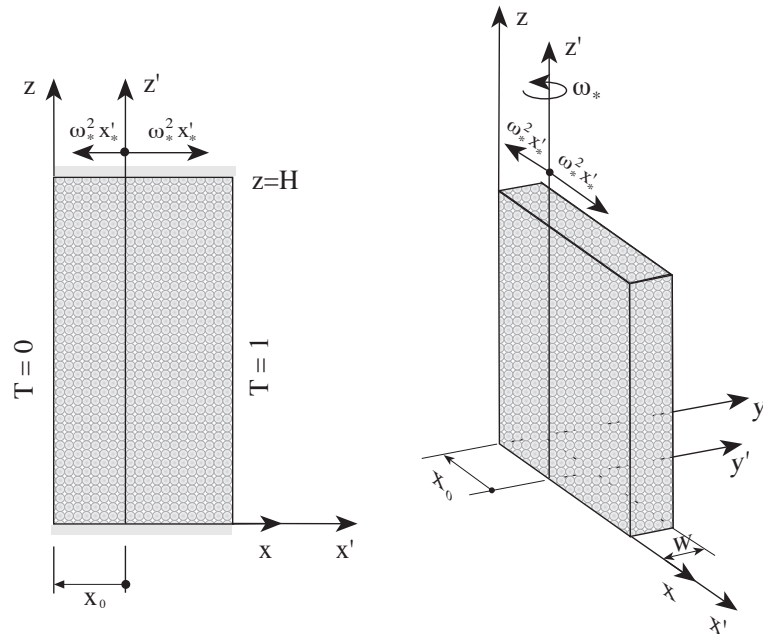


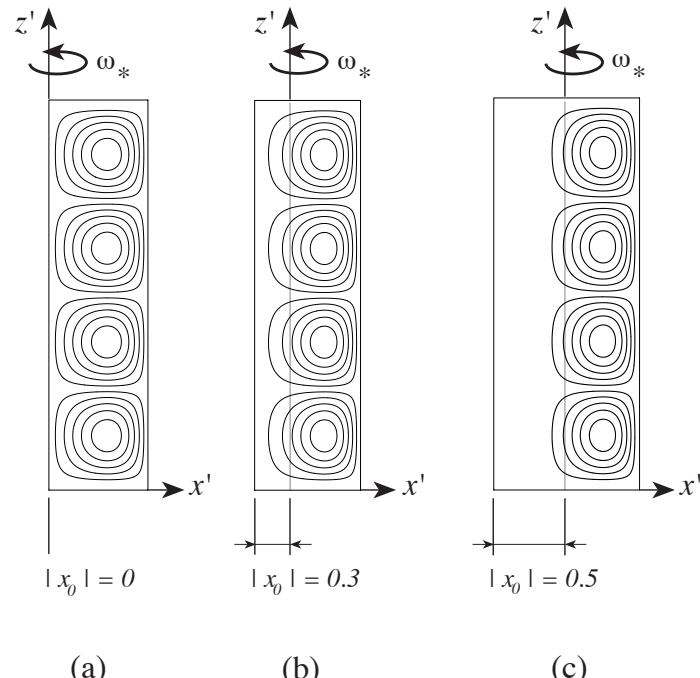
Figure 7: Different transitions in natural convection in a rotating porous layer. (courtesy Elsevier Science Ltd.)



508

509 **Figure 8:** A rotating porous layer having the rotation axis within its boundaries and subject to different
 510 temperatures at the sidewalls. (courtesy Elsevier Science Ltd.)

511



512

513 **Figure 9:** The convective flow field at marginal stability for three different values of $|x_0|$; 10 streamlines
 514 equally divided between ψ_{\min} and ψ_{\max} . (courtesy Elsevier Science Ltd.)

515

516

517 It is therefore convenient to explicitly introduce this fact in the problem formulation specifying
 518 explicitly that $x_0 = -|x_0|$. As a result equation (50) can be expressed in the form

$$519 \quad \mathbf{V} = -\nabla p - Ra_\omega [x - |x_0|] T \hat{\mathbf{e}}_x \quad (60)$$

520 The solution for this case is similar to the previous case leading to the same characteristic equation
 521 for R_c at order 2 as obtained previously in equation (53) for $R_{o,c}$, with the only difference
 522 appearing in the different definition of β and γ as follows

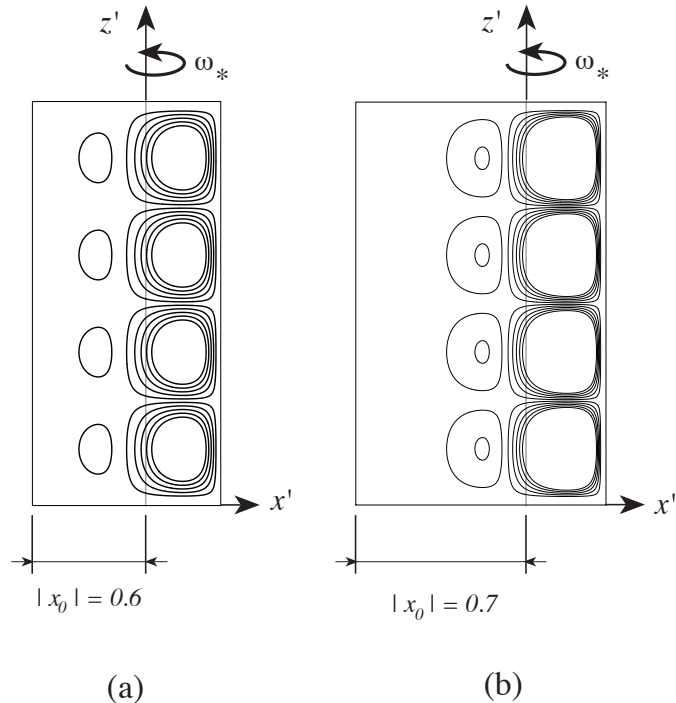
523
$$\beta = \left(\frac{1}{2} - |x_0| \right); \quad \gamma^2 = \frac{256}{81\pi^4} \quad (61)$$

524 The singularity is obtained when $\beta^2 = \gamma^2$, corresponding to $\beta = \gamma$ or $\beta = -\gamma$. Since β is
 525 uniquely related to the offset distance $|x_0|$ and $\gamma = 16/9\pi^2$ is a constant, one can relate the
 526 singularity to specific values of $|x_0|$. At order 2 this corresponds to $|x_0| = 0.3199$ and $|x_0| = 0.680$.
 527 It was shown by Vadasz [41] that the second value $|x_0| = 0.680$ is the only one, which has physical
 528 consequences. This value corresponds to a transition beyond which, i.e., for $|x_0| \geq 0.68$, no positive
 529 roots of R_c exist. It therefore implies an unconditional stability of the basic motionless solution for
 530 all values of R if $|x_0| \geq 0.68$. The transitional value of $|x_0|$ was investigated at higher orders
 531 showing $|x_0| \geq 0.765$ at order 3 and the value increases with increasing the order. The indications
 532 are that as the order increases the transition value of $|x_0|$ tends towards the limit value of 1. The
 533 results for the critical values of the centrifugal Rayleigh number expressed in terms of R_c vs. $|x_0|$
 534 are presented graphically by Vadasz [41], who concluded that increasing the value of $|x_0|$ has a
 535 stabilizing effect. The results for the convective flow field as obtained by Vadasz [41] are presented
 536 in Figures 9, 10 and 11 for different values of $|x_0|$. Keeping in mind that to the right of the rotation
 537 axis the centrifugal acceleration has a destabilizing effect while to its left a stabilizing effect is
 538 expected; the results presented in Figures 9(b) and (c) reaffirm this expectation showing an eccentric
 539 shift of the convection cells towards the right side of the rotation axis. When the rotation axis is
 540 moved further towards the hot wall, say at $|x_0| = 0.6$ as presented in Figure 10(a), weak convection
 541 cells appear even to the left of the rotation axis. This weak convection becomes stronger as $|x_0|$
 542 increases, as observed in Figure 10(b) for $|x_0| = 0.7$ and formation of boundary layers associated
 543 with the primary convection cells is observed to the right of the rotation axis. These boundary
 544 layers become more significant for $|x_0| = 0.8$ as represented by sharp streamlines gradients in
 545 Figure 11(a). When $|x_0| = 0.9$ Figure 11(b) shows that the boundary layers of the primary
 546 convection are well established and the whole domain is filled with weaker secondary, tertiary and
 547 further convection cells. The results for the isotherms corresponding to values of
 548 $|x_0| = 0, 0.5, 0.6$ and 0.7 are presented in Figure 12 where the effect of moving the axis of rotation
 549 within the porous layer, on the temperature is evident.

550 Previously the discussion focused on centrifugally driven natural convection under conditions
 551 of small rotation rates, i.e. $Ek \gg 1$. Then, as a first approximation the Coriolis effect was neglected.
 552 In this section the effect of the Coriolis acceleration on natural convection is presented even when
 553 this effect is small, i.e., $Ek \gg 1$. A long rotating porous box where the temperature gradient was
 554 perpendicular to the centrifugal body force was considered by Vadasz [35]. The possibility of
 555 internal heat generation was included but the case without heat generation, i.e., when the box is
 556 heated from above and cooled from below was dealt with separately. The leading order basic flow
 557 was evaluated analytically. From the solutions it was concluded that the Coriolis effect on natural
 558 convection is controlled by the combined dimensionless group

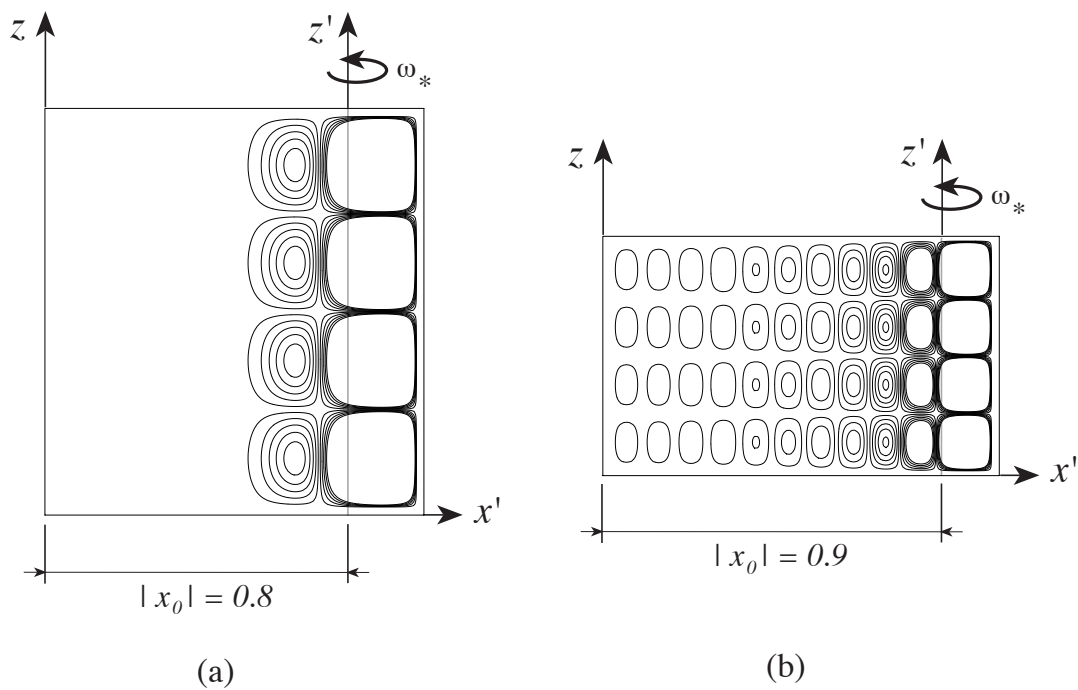
559
$$\sigma = \frac{Ra_\omega}{Ek} = \frac{2\beta_{T^*} \Delta T_c \omega_*^3 L_* H_* K_o^2}{\alpha_{e^*} v_*^2 \phi} \quad (62)$$

560 The flow and temperature fields in the plane $y-z$, perpendicular to the leading order natural
 561 convection plane as evaluated through the analytical solution shows single or double vortices
 562 secondary flow in this plane, perpendicular to the basic flow.
 563



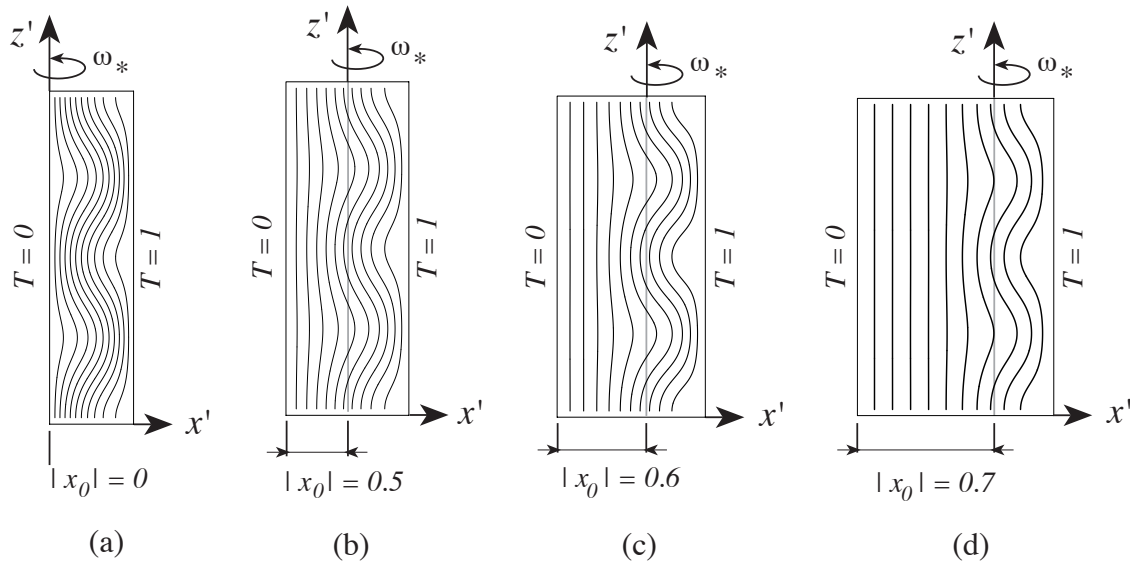
564

565 **Figure 10:** The convective flow field at marginal stability for two different values of $|x_0|$; 10 streamlines
 566 equally divided between ψ_{\min} and ψ_{\max} . (courtesy Elsevier Science Ltd.)
 567



568

569 **Figure 11:** The convective flow field at marginal stability for two different values of $|x_0|$; 10 streamlines
 570 equally divided between ψ_{\min} and ψ_{\max} . (courtesy Elsevier Science Ltd.)
 571

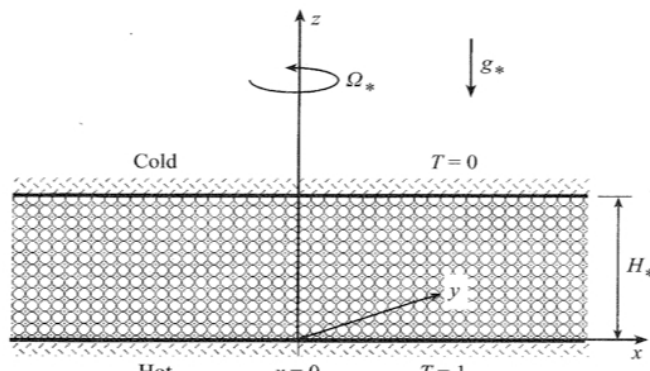


572

573 **Figure 12:** The convective temperature field at marginal stability for four different values of $|x_0|$; 10 isotherms
 574 equally divided between $T_{\min} = 0$ and $T_{\max} = 1$. (courtesy Elsevier Science Ltd.)
 575

576 **5. Coriolis Effect on Natural Convection due to Gravity Buoyancy**

577 The problem of a rotating porous layer subject to gravity and heated from below (see Figure
 578 13) was originally investigated by Friedrich [75] and by Patil and Vaidyanathan [17]. Both studies
 579 considered a non-Darcy model, which is probably subject to the limitations as shown by Nield [68].
 580 Friedrich [74] focused on the effect of Prandtl number on the convective flow resulting from a linear
 581 stability analysis as well as a non-linear numerical solution, while Patil and Vaidyanathan [17] dealt
 582 with the influence of variable viscosity on the stability condition. The latter concluded that variable
 583 viscosity has a destabilizing effect while rotation has a stabilizing effect. Although the non-Darcy
 584 model considered included the time derivative in the momentum equation the possibility of
 585 convection setting-in as an oscillatory instability was not explicitly investigated by Patil and
 586 Vaidyanathan [17]. It should be pointed out that for a pure fluid (non-porous domain) convection
 587 sets in as oscillatory instability for a certain range of Prandtl number values (Chandrasekhar [76,
 588 77]). This possibility was explored by Friedrich [75], which presents stability curves for both
 589 monotonic and oscillatory instability. Jou and Liaw [19] investigated a similar problem of gravity
 590 driven thermal convection in a rotating porous layer subject to transient heating from below. By
 591 using a non-Darcy model they established the stability conditions for the marginal state without
 592 considering the possibility of oscillatory convection.



593

594 **Figure 13:** A rotating fluid saturated porous layer heated from below. (courtesy: Cambridge University Press.)
 595

596 An important analogy was discovered by Palm and Tyvand [20] who showed, by using a Darcy
 597 model, that the onset of gravity driven convection in a rotating porous layer is equivalent to the
 598 case of an anisotropic porous medium. The critical Rayleigh number was found to be

$$599 \quad Ra_{g,cr} = \pi^2 \left[(1+Ta)^{1/2} + 1 \right]^2 \quad (63)$$

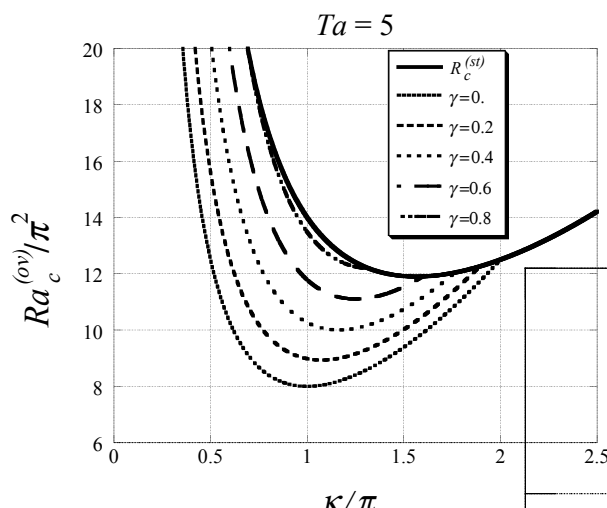
600 where Ta is the Taylor number defined here as

$$601 \quad Ta = \left(\frac{2\omega_* K_o}{\phi v_*} \right)^2 \quad (64)$$

602 and the corresponding critical wave number is $\pi(1+Ta)^{1/4}$. The porosity is missing in Palm and
 603 Tyvand [20] definition of Ta . Nield [21, 22] has pointed out that these authors and others have
 604 omitted the porosity from the Coriolis term. This result, eq. (63) (amended to include the correct
 605 definition of Ta), was confirmed by Vadasz [41] for a Darcy model extended to include the time
 606 derivative term (see equation (31) with $Ra_\omega = 0$), while performing linear stability as well as a
 607 weak non-linear analyses of the problem to provide differences as well as similarities with the
 608 corresponding problem in pure fluids (non-porous domains). As such, Vadasz [42] found that, in
 609 contrast to the problem in pure fluids, overstable convection in porous media at marginal stability
 610 is not limited to a particular domain of Prandtl number values (in pure fluids the necessary
 611 condition is $Pr < 1$). Moreover, it was also established by Vadasz [42] that in the porous media
 612 problem the critical wave number in the plane containing the streamlines for stationary convection
 613 is not identical to the critical wave number associated with convection without rotation, and is
 614 therefore not independent of rotation, a result which is quite distinct from the corresponding
 615 pure-fluids problem. Nevertheless, it was evident that in porous media, just as in the case of pure
 616 fluids subject to rotation and heated from below, the viscosity at high rotation rates has a
 617 destabilizing effect on the onset of stationary convection, i.e. the higher the viscosity the less stable
 618 is the fluid. An example of stability curves for overstable convection is presented in Figure 14 for
 619 $Ta = 5$, where κ is the wave number. The upper bound of these stability curves is represented by
 620 a stability curve corresponding to stationary convection at the same particular value of the Taylor
 621 number, while the lower bound was found to be independent of the value of Taylor number and
 622 corresponds to the stability curve for overstable convection associated with $Va = 0$.

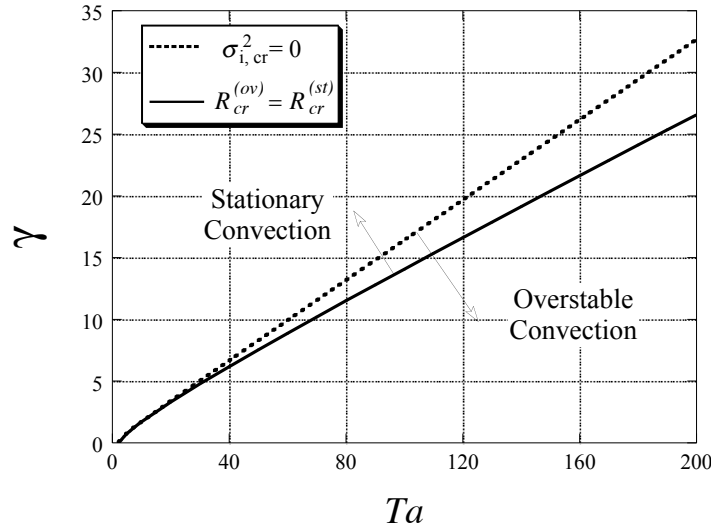
623

624



625

626 **Figure 14:** Stability curves for overstable gravity driven convection in a rotating porous layer heated from
 627 below ($\gamma = Va/\pi^2$, $R = Ra_s/\pi^2$). (courtesy: Cambridge University Press.)
 628



629

630 **Figure 15:** Stability map for gravity driven convection in a rotating porous layer heated from below
 631 $(\gamma = Va/\pi^2, R = Ra_g/\pi^2)$. (courtesy: Cambridge University Press.)

632

633 Two conditions have to be fulfilled for overstable convection to set in at marginal stability, i.e., (i)
 634 the value of Rayleigh number has to be higher than the critical Rayleigh number associated with
 635 overstable convection, and (ii) the critical Rayleigh number associated with overstable convection
 636 has to be smaller than the critical Rayleigh number associated with stationary convection. The
 637 stability map obtained by Vadasz [42] is presented in Figure 15, which shows that the $Ta - \gamma$
 638 ($\gamma = Va/\pi^2$) plane is divided by a continuous curve (almost a straight line) into two zones, one for
 639 which convection sets in as stationary, and the other where overstable convection is preferred. The
 640 dotted curve represents the case when the necessary condition (i) above is fulfilled but condition (ii)
 641 is not. Weak non-linear stationary as well as oscillatory solutions were derived, identifying the
 642 domain of parameter values consistent with supercritical pitchfork (in the stationary case) and Hopf
 643 (in the oscillatory case) bifurcations. Unfortunately due to a typo affecting the sign of one of the
 644 nonlinear terms in the weak nonlinear analysis the direction of the bifurcations presented seems to
 645 be incorrect. The identification of the tricritical point corresponding to the transition from
 646 supercritical to subcritical bifurcations was presented on the $\gamma - Ta$ parameter plane. The
 647 possibility of a codimension-2 bifurcation, which is anticipated at the intersection between the
 648 stationary and overstable solutions, although identified as being of significant interest for further
 649 study, was not investigated by Vadasz [42].

650

651 6. Natural Convection due to Combined Centrifugal and Gravity Buoyancy

652 Previous sections dealt with natural convection due to centrifugal buoyancy, when the gravity
 653 body force contribution was negligible, $Ra_g = 0$, satisfying the condition: $Ra_g/Ra_\omega = g_*/\omega_*^2 L_* \ll 1$,
 654 or with gravity buoyancy when the centrifugal body force contribution was insignificant, $Ra_\omega = 0$,
 655 satisfying the condition: $Ra_\omega/Ra_g = \omega_*^2 L_*/g_* \ll 1$. In the present section the focus is on conditions
 656 when both centrifugal buoyancy as well as gravity buoyancy effects are significant, $Ra_g \sim Ra_\omega$, but
 657 at small rotation rates, i.e. $Ek \gg 1$. Then, as a first approximation the Coriolis effect can be
 658 neglected. Figure 4 still applies to the present problem, subject to a slight modification of drawing
 659 the gravity acceleration g_* in the negative z direction. The notation remains the same and
 660 equation (50) becomes

$$661 \quad \mathbf{V} = -\nabla p - Ra_{\omega\phi} [1 + \eta x] T \hat{\mathbf{e}}_x + Ra_g T \hat{\mathbf{e}}_z \quad (65)$$

662 where $\eta = 1/x_0 = Ra_\omega / Ra_{\omega_0}$ represents the reciprocal of the offset distance from the axis of rotation.
 663 The approach being the same as before, the solution is expressed as a sum of a basic solution and
 664 small perturbations as presented in equation (52). However, because of the presence of the gravity
 665 component in equation (65), a motionless conduction solution is not possible any more. Therefore,
 666 the basic solution far from the top and bottom walls is obtained in the form

$$667 \quad u_b = v_b = 0; \quad w_b = Ra_g \left(x - \frac{1}{2} \right); \quad T_b = x; \quad p_b = \frac{1}{2} Ra_g z - Ra_{\omega_0} x^2 \left[\frac{1}{2} + \frac{1}{3} \eta x \right] + \text{const.} \quad (66)$$

668 Substituting this basic solution into the governing equations and linearizing the result by neglecting
 669 terms that include products of perturbations, which are small, yields a set of partial differential
 670 equations for the perturbations. Assuming a normal modes expansion in the y and z directions
 671 in the form

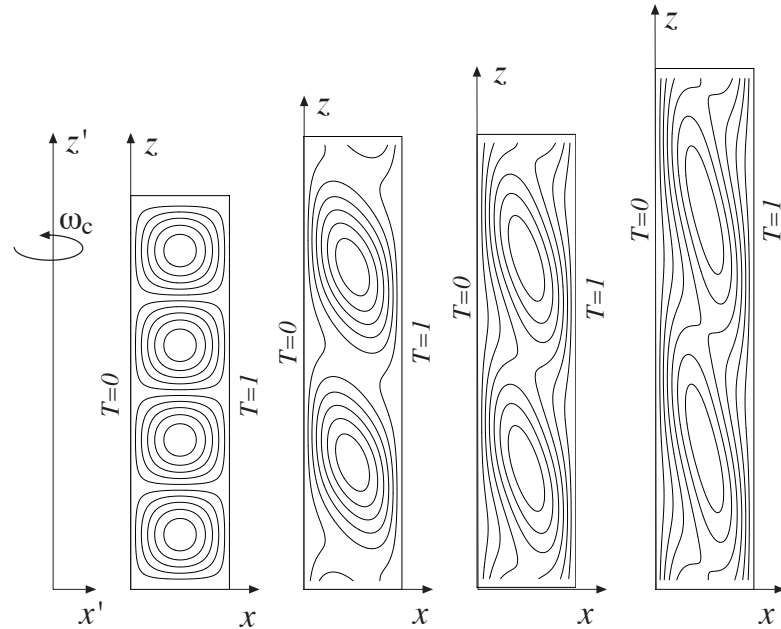
$$672 \quad T' = A_\kappa \theta(x) \exp[\sigma t + i(\kappa_y y + \kappa_z z)] \quad (67)$$

673 where κ_y and κ_z are the wave numbers in y and z directions respectively, i.e., $\kappa^2 = \kappa_y^2 + \kappa_z^2$,
 674 and using the Galerkin method, the following set of linear algebraic equations is obtained at
 675 marginal stability (i.e., for $\sigma = 0$)

$$676 \quad \sum_{m=1}^M \left\{ \left[2(m^2 \pi^2 + \kappa^2)^2 - \kappa^2 Ra_{\omega_0} (2 + \eta) \right] \delta_{ml} + \right. \\ 677 \quad \left. \left[\frac{16ml\kappa^2 Ra_{\omega_0}}{\pi^2(l^2 - m^2)} - i \frac{8ml\kappa_z Ra_g}{\pi^2(l^2 - m^2)^2} [\pi^2(l^2 + m^2) + 2\kappa^2] \right] \delta_{m+l, 2p-1} \right\} a_m = 0 \quad (68)$$

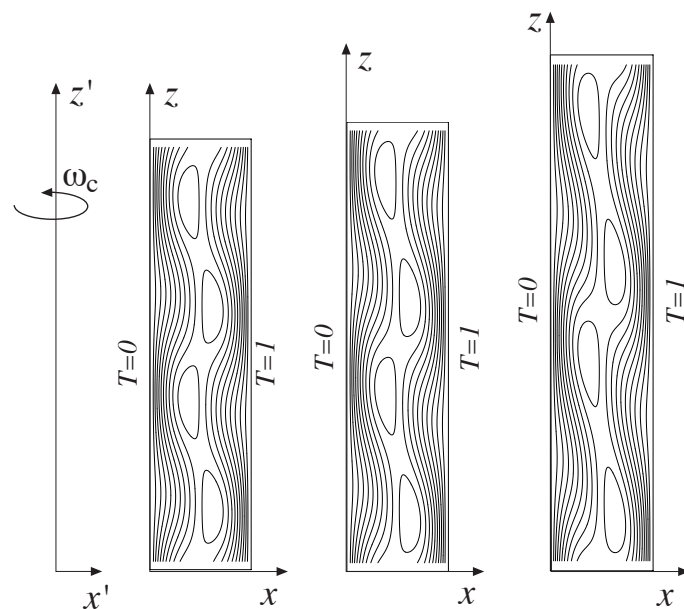
678 for $l = 1, 2, 3, \dots, M$ and $i = \sqrt{-1}$. In equation (68) δ_{ml} is the Kronecker delta function and the
 679 index p can take arbitrary integer values, since it stands only for setting the second index in the
 680 Kronecker delta function to be an odd integer. A particular case of interest is the configuration
 681 when the layer is placed far away from the axis of rotation, i.e. when the length of the layer L_* is
 682 much smaller than the offset distance from the rotation axis x_0 . Therefore for $x_0 = (x_{0*}/L_*) \rightarrow \infty$
 683 or $\eta \rightarrow 0$ the contribution of the term ηx in equation (65) is not significant. Substitution of this
 684 limit into equation (68) and solving the system at the second order, i.e. $M = 2$, yields a quadratic
 685 equation for the characteristic values of Ra_{ω_0} . This equation has no real solutions for values of
 686 $\alpha = \kappa_z^2 / \pi^2$ beyond a transitional value $\alpha_r = (27\pi^3 / 16 Ra_g)^2$. This value was evaluated at higher
 687 orders too, showing that for $M = 10$ the transitional value varies very little with Ra_g , beyond a
 688 certain Ra_g value around 50π . The critical values of Ra_{ω_0} were evaluated for different values of
 689 R_g ($= Ra_g / \pi$) and the corresponding two-dimensional convection solutions in terms of streamlines
 690 are presented graphically for the odd modes in Figure 16(a), showing the perturbation solutions in
 691 the $x-z$ plane as skewed convection cells when compared with the case without gravity. The
 692 corresponding convection solutions for the even modes are presented in Figure 16(b), where it is
 693 evident that the centrifugal effect is felt predominantly in the central region of the layer, while the
 694 downwards and upwards basic gravity driven convection persists along the left and right
 695 boundaries, respectively, although not in straight lines. Beyond the transition value of α , the basic
 696 gravity driven convective flow (equation (66)) is unconditionally stable. These results were shown
 697 to have an analogy with the problem of gravity driven convection in a non-rotating, inclined porous
 698 layer (Govender and Vadasz [29]). Qualitative experimental confirmation of these results was
 699 presented by Vadasz and Heerah [45] by using a thermo-sensitive liquid-crystal tracer in a rotating
 700 Hele-Shaw cell. When the layer is placed at an arbitrary finite distance from the axis of rotation no
 701 real solutions exist for the characteristic values of Ra_{ω_0} corresponding to any values of γ other
 702 than $\gamma = \kappa_z Ra_g = 0$. In the presence of gravity $Ra_g \neq 0$, and $\gamma = 0$ can be satisfied only if $\kappa_z = 0$.
 703 Therefore the presence of gravity in this case has no other role but to exclude the vertical modes of
 704 convection. The critical centrifugal Rayleigh numbers and the corresponding critical wave numbers

705 are the same as in the corresponding case without gravity as presented in section 4.3. However, the
 706 eigenfunctions representing the convection pattern are different as they exclude the vertical modes
 707 replacing them with a corresponding horizontal mode in the y direction. Therefore, a cellular
 708 convection in the $x - y$ plane is superimposed to the basic convection in the $x - z$ plane.
 709



710 (a) $R_g = 0$ $R_g = 5$ $R_g = 10$ $R_g = 20$

711



712 (b) $R_g = 5$ $R_g = 10$ $R_g = 20$

713 **Figure 16:** The convective flow field (streamlines) at marginal stability for different values of R_g ($= Ra_g / \pi$);
 714 (a) the odd modes; (b) the even modes.
 715
 716

717 **7. Additional Effects on Flow and Natural Convection in Rotating Porous Media**

718 Not much research results are available for thermo-haline convection in porous media subject
719 to rotation. Chakrabarti and Gupta [78] investigated a non-Darcy model, which includes the
720 Brinkman term as well as a non-linear convective term in the momentum equation (in the form
721 $(V \cdot \nabla) V$). Therefore the model's validity is subject to the limitations pointed out by Nield [69]. Both
722 linear and non-linear analyses were performed and overstability was particularly investigated.
723 Overstability is affected in this case by both the presence of a salinity gradient and by the Coriolis
724 effect. Apart from the thermal and solutal Rayleigh numbers and the Taylor number, two
725 additional parameters affect the stability. These are the Prandtl number $Pr = v_* / \alpha_{e^*}$, and the Darcy
726 number $Da = K_o / H_*^2$, where H_* is the layer's height. The authors found that, in the range of
727 values of the parameters, which were considered, the linear stability results favor setting-in of
728 convection through a mechanism of overstability. The results for non-linear steady convection show
729 that the system becomes unstable to finite amplitude steady disturbances before it becomes
730 unstable to disturbances of infinitesimal amplitude. Thus the porous layer may exhibit subcritical
731 instability in the presence of rotation. These results are surprising at least in the sense of their
732 absolute generality and the authors mention that further confirmation is needed in order to increase
733 the degree of confidence in these results. A similar problem was investigated by Rudraiah et al [16]
734 while focusing on the effect of rotation on linear and non-linear double-diffusive convection in a
735 sparsely packed porous medium. A non-Darcy model identical to the one used by Chakrabarti and
736 Gupta [78] was adopted by Rudraiah et al [16], however the authors spelled out explicitly that the
737 model validity is limited to high porosity and high permeability which makes it closer to the
738 behavior of a pure fluid system (non-porous domain). It is probably for this reason that the authors
739 preferred to use the non-porous medium definitions for Rayleigh and Taylor numbers which differ
740 by a factor of Da and Da^2 , respectively, from the corresponding definitions for porous media. It
741 is because of these definitions that the authors concluded that for small values of Da number the
742 effect of rotation is negligible for values of $Ta < 10^6$. This means that rotation has a significant effect
743 for large rotation rates, i.e., $Ta > 10^6$. If the porous media Taylor number had been used instead,
744 i.e., the proper porous media scales, then one could have significant effects of rotation at porous
745 media Taylor numbers as small as $Ta > 10$. Hence, the results presented by Rudraiah et al [16] are
746 useful provided $Da = O(1)$ which is applicable for high permeability (or sparsely packed) porous
747 layers. Marginal stability as well as overstability were investigated and the results show different
748 possibilities of existence of neutral curves by both mechanisms, i.e., monotonic as well as oscillatory
749 instability. In this regard the results appear more comprehensive in the study by Rudraiah et al [16]
750 than in Chakrabarti and Gupta [78]. The finite amplitude analysis was performed by using a
751 severely truncated representation of a Fourier series for the dependent variables. As a result a
752 seventh-order Lorenz model of double diffusive convection in a porous medium in the presence of
753 rotation was obtained. From the study of steady, finite amplitude analysis the authors found that
754 subcritical instabilities are possible, depending on the parameter values. The effect of the
755 parameters on the heat and mass transport was investigated as well, and results presenting this
756 effect are discussed in Rudraiah et al [16]. The onset of double-diffusive convection in a rotating
757 porous layer was investigated by Lombardo and Mulone [60], Malashetty, Pop, and Heera [48],
758 Falsaperla, Giacobbe and Mulone [63]. Triple-diffusion effects in rotating porous layers were
759 investigated by Capone and De Luca [64]. They evaluated the ultimate boundedness of the
760 solutions and found a necessary and sufficient condition for the global nonlinear asymptotic
761 L^2 -stability of the motionless conduction solution.

762 Lack of local thermal equilibrium (LaLotheq) or local thermal non-equilibrium (LTNE) means
763 that distinct temperature values exist between the solid and fluid phases within the same
764 Representative Elementary Volume (REV). Malashetty et al [53] presented the linear stability and
765 the onset of convection in a porous layer heated from below and subject to rotation, accounting for
766 the Coriolis effect as in Vadasz [42] but allowing for distinct temperature values between the solid
767 and fluid phases, i.e. lack of local thermal equilibrium (LaLotheq), or local thermal non-equilibrium

(LTNE). The nonlinear part of the analysis was undertaken by using a truncated mode spectral system, such as the one used by Vadasz and Olek [46] but adapted for the LaLotheq conditions. The effect of finite heat transfer between the phases leading to lack of local thermal equilibrium was investigated also by Govender and Vadasz [32] while investigating also the effect of mechanical and thermal anisotropy on the stability of a rotating porous layer heated from below and subject to gravity. The topic of anisotropic effects is discussed in the next section. Bhaduria [47] investigated the effect of temperature modulation on the onset of thermal instability in a horizontal fluid-saturated porous layer heated from below and subject to uniform rotation. An extended Darcy model, which includes the time derivative term, has been considered, and a time-dependent periodic temperature field was applied to modulate the surfaces' temperature. A perturbation procedure based on small amplitude of the imposed temperature modulation was used to study the combined effect of rotation, permeability, and temperature modulation on the stability of the fluid saturated porous layer. The correction of the critical Rayleigh number was calculated as a function of amplitude and frequency of modulation, the porous media Taylor number, and the Vadasz number. It was found that both rotation and permeability suppress the onset of thermal instability. Furthermore, the author concluded that temperature modulation could either promote or retard the onset of convection.

The effect of anisotropy on the stability of convection in a rotating porous layer subject to centrifugal body forces was investigated by Govender [25]. The Darcy model extended to include anisotropic effects and rotation was used to describe the momentum balance and a modified energy equation that included the effects of thermal anisotropy was used to account for the heat transfer. The linear stability theory was used to evaluate the critical Rayleigh number for the onset of convection in the presence of thermal and mechanical anisotropy. It was found that the convection was stabilized when the thermal anisotropy ratio (which is a function of the thermal and mechanical anisotropy parameters) increased in magnitude. Malashetty and Swamy [54], and Govender and Vadasz [32] investigated the Coriolis effect on natural convection in a rotating anisotropic fluid-saturated porous layer heated from below and subject to gravity as the body force. Malashetty and Swamy [54] assumed local thermal equilibrium while Govender and Vadasz [32] dealt with lack of local thermal equilibrium (LaLotheq), or local thermal non-equilibrium (LTNE). Malashetty and Swamy [54] used the linear stability theory as well as a nonlinear spectral method. The linear theory was based on the usual normal mode technique and the nonlinear theory on a truncated Galerkin analysis. The Darcy model extended to include a time derivative and the Coriolis terms with an anisotropic permeability was used to describe the flow through the porous media. A modified energy equation including the thermal anisotropy was used. The effect of rotation, mechanical and thermal anisotropy parameters and the Prandtl number on the stationary and overstable convection was discussed. It was found that the effect of mechanical anisotropy is to prefer the onset of oscillatory convection instead of the stationary one. It was also found, just as in Vadasz [42], that the existence of overstable motions in case of rotating porous media is not restricted to a particular range of Prandtl number as compared to the pure viscous fluid case. The steady finite amplitude analysis was performed using the truncated Galerkin modes to find the Nusselt number. The effect of various parameters on heat transfer was investigated. Govender and Vadasz [32] analyzed the stability of a horizontal rotating fluid saturated porous layer exhibiting both thermal and mechanical anisotropy, subject to lack of local thermal equilibrium (LaLotheq), or local thermal non-equilibrium (LTNE). All of the results were presented as a function of the scaled inter-phase heat transfer coefficient. The results of the linear stability theory have revealed that increasing the conductivity ratio and the mechanical anisotropy has a destabilizing effect, whilst increasing the fluid and solid thermal conductivity ratios is stabilizing. In general it was found that rotation has a stabilizing effect in a porous layer exhibiting mechanical or thermal (or both mechanical and thermal) anisotropy. Additional results for the effect of rotation on thermal convection in an anisotropic porous medium were presented by Vanishree and Siddheshwar [49].

An interesting, more recent, application is related to nanofluids. A nanofluid is a suspension of nanoparticles or nanotubes in a liquid. When the liquid is saturating a porous matrix one deals with

nanofluids in porous media. Chand and Rana [79] analyzed the Coriolis effect on natural convection in a rotating porous layer saturated by a nanofluid. Agarwal and Bhaduria [52], Rana and Agarwal [55], investigated the natural convection in a rotating porous layer saturated by a nanofluid and a binary mixture. This implies that the nanoparticles are suspended in a binary mixture, e.g. in a water and salt solution. Therefore double-diffusive convection is anticipated. The model used for the nanofluid incorporates the effects of Brownian motion and thermophoresis, while the Darcy model is used for the porous medium. The neutral and critical Rayleigh numbers for stationary and oscillatory convection have been obtained in terms of various dimensionless parameters. The authors concluded that the principle of exchange of stabilities is applicable in the present problem, while more amount of heat is required in the nanofluid case for convection to set-in. Agarwal et al [50] considered the convection in a rotating anisotropic porous layer saturated by a nanofluid. The model used for nanofluid combines the effect of Brownian motion along with thermophoresis, while for a porous medium the Darcy model has been used. Using linear stability analysis the expression for the critical Rayleigh number has been obtained in terms of various dimensionless parameters. Agarwal et al [50] indicate that bottom-heavy and top-heavy arrangements of nanoparticles tend to prefer oscillatory and stationary modes of convection, respectively. The onset of double-diffusive nanofluid convection in a rotating porous layer was investigated by Yadav et al [56].

During solidification of binary alloys the solidification front between the solid and the liquid phases is not a sharp front but rather a mushy layer combining liquid and solid phases each one being interconnected. It is not surprising therefore that the treatment of this mushy layer follows all the rules applicable to a porous medium. Natural convection due to thermal as well as concentration gradients occurs in the mushy layer resulting in possible creation of freckles that might affect the quality of the cast. When such a process occurs in a system that is subject to rotation, centrifugal buoyancy as well as Coriolis effects are relevant and essential to be included in any model of this process. Govender and Vadasz [31] investigated such a system via a weak nonlinear analysis for moderate Stefan numbers applicable to stationary convection in a rotating mushy layer. Consequently Govender and Vadasz [30] investigated a similar system via a weak nonlinear analysis for moderate Stefan numbers applicable to oscillatory convection in a rotating mushy layer. A near-eutectic approximation and large far-field temperature were employed in both papers in order to decouple the mushy layer from the overlying liquid melt. The parameter regimes in terms of Taylor number for example where the bifurcation is subcritical or supercritical were identified. In the case of oscillatory convection increasing the Taylor number lead to a supercritical bifurcation.

Linear stability was the primary method used in previous sections to establish the stability criteria for the onset of natural convection in a rotating porous layer. Straughan [73] pioneered the introduction of a nonlinear analysis producing a sharp nonlinear stability threshold in rotating porous convection. The application and generalization of this method was presented by Lombardo and Mulone [60], while deriving necessary and sufficient conditions of global nonlinear stability for double-diffusive convection in rotating porous media. The nonlinear method was expanded and summarized by Straughan [59]. The application of this nonlinear method to natural convection in non-rotating porous media was expanded showing the coincidence between linear and global nonlinear stability of non-constant through-flows was presented by Capone and De Luca [66] by using the “Rionero Auxiliary System Method”. Weak nonlinear solutions were presented by Bhaduria et al [51]. Investigations into the effects of inertia on rotating porous convection were undertaken by Falsaperla, Mulone, and Straughan [62], and by Capone and Rionero [65]. The latter used again the “Rionero Auxiliary System Method” to derive a set of conditions for the significance of inertia in this problem and for global nonlinear stability in terms of the porous media Taylor number as well as Vadasz number.

Other studies considered effects of rotation for a combination of previously presented conditions. For example Capone and Gentile [80] presented sharp stability results in a rotating anisotropic porous layer subject to lack of local thermal equilibrium (LaLotheq, LTNE). Double

872 diffusive convection in a rotating anisotropic porous layer was presented by Galkwad and Kouser
873 [81], Malashetty and Heera [82], and Malashetty and Begum [83]. Double diffusive convection in a
874 rotating porous medium saturated with a coupled stress fluid was considered by Malashetty et al
875 [84], while double diffusive convection in a rotating porous layer saturated by a viscoelastic fluid
876 was investigated by Kumar and Bhaduria [85]. The effect of rotation on a micropolar
877 ferromagnetic fluid heated from below saturating a porous medium was presented by Sunil et al
878 [86]. Rotation effects on convection in a porous layer saturated by nanofluids was further
879 considered by Bhaduria and Agrawal [87], for a porous medium model including the Brinkman
880 term. A similar model was presented by Yadav and Lee [88] for the case of lack of local thermal
881 equilibrium (LaLotheq, LTNE), and by Yadav et al [89] for a Darcy model Soret driven convection
882 in a rotating porous medium saturated by a nanofluid. Brinkman convection induced by internal
883 heating in a rotating porous medium layer saturated by a nanofluid was investigated by Yadav et al
884 [90], while thermal instability in a rotating porous layer saturated by a non-Newtonian nanofluid
885 was considered by Yadav et al [91]. Yadav et al [92] presented the conditions for the onset of
886 convection in a rotating porous layer due internal heating by using a Brinkman model. The effects
887 of thermal modulation, i.e. top and bottom imposed temperatures are allowed to vary slightly in
888 time, were considered by Malashetty and Swamy [93] using a Darcy model and Bhaduria [94]
889 using a Brinkman model. A similar Brinkman model was applied for investigating the effects of
890 centrifugal buoyancy in a rotating porous layer far away from the center of rotation subject to
891 modulation of rotation by Om et al [95], i.e. the angular velocity was allowed to slightly vary
892 periodically in time. The same conditions applied to a rotating porous layer distant an arbitrary
893 distance from the center of rotation was presented by Om et al [96]. Coriolis effect on thermal
894 convective instability of viscoelastic fluids in a rotating porous cylindrical annulus was investigated
895 by Kang et al [97]. Küppers-Lortz instability in rotating Rayleigh-Benard convection in a porous
896 medium was studied by Rameshwar et al. [98].

897

898

8. Conclusions

899 A review of the variety of instability problems linked to natural convection in rotating porous
900 media was presented. The effect of centrifugal buoyancy was investigated separately, and later in
901 combination with gravitational buoyancy. The cases when the Coriolis effect is significant were also
902 analyzed and the corresponding results were discussed. The diversity of additional effects linked to
903 natural convection in rotating porous media, such as thermo-solutal and double-diffusive
904 convection, the effect of anisotropy of the porous medium, the inclusion of nanofluids in rotating
905 porous media, solidification of binary alloys, and lack of local thermal equilibrium are examples
906 that were also shortly reviewed. The pioneering studies on global nonlinear analyses and
907 investigations of the effect of inertia on natural convection in rotating porous media concluded the
908 present review.

909

910 **Author Contributions:** N/A911 **Conflicts of Interest:** "The author declares no conflict of interest.".

912

913

References

1. Fowler, A.C. A compaction model for melt transport in the earth asthenosphere Part I: The base model. In *Magma Transport and Storage*, ed. Michael P. Raya, John Wiley & Sons, Chichester, 1990, pp. 3-14.
2. Vadasz, P., Fluid Flow and Thermal Convection in Rotating Porous Media. In *Handbook of Porous Media*, Kambiz Vafai (ed.), Marcel Dekker, New York, Basel, 2000, pp. 395-439.

918 3. Vadasz, P. *Fluid Flow and Heat Transfer in Rotating Porous Media*, Springer (Springer Briefs in applied
919 Science and Engineering, series editor: F.A. Kulacki), Cham, Heidelberg, New York, Dordrecht, London,
920 2016.

921 4. Vadasz, P. Natural Convection in Rotating Flows, in *Handbook of Thermal Science and Engineering*, F. A.
922 Kulacki (ed.), Chapter 11, Springer International Publishing AG, 2018, pp. 691-758.

923 5. Nield, D.A.; Bejan, A. *Convection in Porous Media*, 4th edition, Springer, New York, Heidelberg, Dordrecht,
924 London, 2013.

925 6. Nield, D.A.; Bejan, A. *Convection in Porous Media*, 5th edition, Springer, New York, Heidelberg, Dordrecht,
926 London, 2017.

927 7. Bejan, A. *Convection Heat Transfer*, 4th edition, John Wiley & Sons, Hoboken, New Jersey, 2013.

928 8. Dagan, G. Some aspects of heat and mass transfer in porous media. In *Fundamentals of Transport
929 Phenomena in Porous Media* (ed. J. Bear), Int. Association for Hydraulic Research, Elsevier, New York, 1972,
930 pp. 55-64.

931 9. Acharya, S. Single-phase convective heat transfer: Fundamental equations and foundational assumptions.
932 In *Handbook of Thermal Science and Engineering*, (ed. F. A. Kulacki), Springer, 2017.

933 10. Wiesche, S. Heat Transfer in Rotating Flows, in *Handbook of Thermal Science and Engineering*, (ed. F. A.
934 Kulacki), Springer, 2017.

935 11. Vadasz, P. Fundamentals of Flow and Heat Transfer in Rotating Porous Media. In *Heat Transfer PA 5*,
936 Taylor and Francis, Bristol, 1994, pp. 405-410.

937 12. Vadasz, P. Flow in rotating porous media. In *Fluid Transport in Porous Media* from the series *Advances in
938 Fluid Mechanics* 13, ed. P. du Plessis & series ed. M. Rahman, Computational Mechanics Publications,
939 Southampton, 1997, pp. 161-214.

940 13. Vadasz, P. Free convection in rotating porous media. In *Transport Phenomena in Porous Media*, ed. D.B.
941 Ingham and I. Pop, Elsevier Science, Oxford, 1998, pp. 285-312.

942 14. Vadasz, P. Heat Transfer and Fluid Flow in Rotating Porous Media. In *Computational Methods in Water
943 Resources 1*, S.M. Hassanzadeh, R.J. Schotting, W.G. Gray & G.F. Pinder (eds.), *Development in Water
944 Science* 47, Elsevier, Amsterdam, 2002, pp. 469-476.

945 15. Vadasz, P. Thermal Convection in Rotating Porous Media. in *Trends in Heat, Mass & Momentum Transfer 8*,
946 Research Trends, Trivandrum, Kerala, India, 2002, pp. 25-58.

947 16. Rudraiah, N.; Shivakumara, I.S.; and Friedrich, R. The effect of rotation on linear and non-linear
948 double-diffusive convection in a sparsely packed porous medium. *Int. J. Heat Mass Transfer* **1986**, 29, pp.
949 1301-1317.

950 17. Patil, P.R.; Vaidyanathan, G. On setting up of convection currents in a rotating porous medium under the
951 influence of variable viscosity. *Int. J. Engineering Science* **1983**, 21, pp. 123-130.

952 18. Jou, J.J.; Liaw, J.S. Transient thermal convection in a rotating porous medium confined between two rigid
953 boundaries. *Int. Comm. Heat and Mass Transfer* **1987**, 14, pp. 147-153.

954 19. Jou, J.J.; Liaw, J.S. Thermal convection in a porous medium subject to transient heating and rotation. *Int. J.
955 Heat Mass Transfer* **1987**, 30 pp. 208-211.

956 20. Palm, E.; Tyvand, A. Thermal convection in a rotating porous layer. *J. Appl. Math. & Physics (ZAMP)* **1984**,
957 35, pp. 122-123.

958 21. Nield, D.A. The stability of convective flows in porous media, in *Convective Heat and Mass Transfer in
959 Porous Media*, ed. S. Kakaç, B. Kilkis, F.A., Kulacki & F. Arniç, Kluwer Academic Publ., Dordrecht, 1991a,
960 pp. 79-122.

961 22. Nield DA. Modeling the effect of a magnetic field or rotation on flow in a porous medium: momentum
962 equation and anisotropic permeability analogy. *Int. J. Heat Mass Transfer* **1999**, 42: 3715-3718.

963 23. Auriault, J.L.; Geindreau, C.; Royer, P. Filtration law in rotating porous media. *C.R. Acad. Sci. Paris* **2000**, t.
964 328 Serie II b, pp. 779-784.

965 24. Auriault, J.L.; Geindreau, C.; Royer, P. Coriolis effects on filtration law in rotating porous media.
966 *Transport in Porous Media* **2002**, 48, pp. 315-330.

967 25. Govender, S. On the effect of anisotropy on the stability of convection in rotating porous media. *Transport
968 in Porous Media* **2006**, 64 (4), pp. 413-422.

969 26. Govender, S. Vadasz number influence on vibration in a rotating porous layer placed far away from the
970 axis of rotation. *J. Heat Transfer* **2010**, 132, pp. 112601/1-4.

971 27. Havstad, M.A.; Vadasz, P. Numerical Solution of the Three Dimensional Fluid Flow in a Rotating
972 Heterogeneous Porous Channel, *Int. J. for Numerical Methods in Fluids* **1999**, 31 (2), pp.411-429.

973 28. Vadasz, P.; Havstad, M.A. The Effect of Permeability Variations on the Flow in a Rotating Porous
974 Channel, *ASME J. Fluids Engineering* **1999**, 121 (3), pp. 568-573.

975 29. Govender, S.; Vadasz, P. Centrifugal and gravity driven convection in rotating porous media - An
976 analogy with the inclined porous layer. *ASME-HTD* **1995**, 309, pp. 93-98.

977 30. Govender, S.; Vadasz, P. Weak non-linear analysis of moderate Stefan number oscillatory convection in
978 rotating mushy layers. *Transport in Porous Media* **2002**, 48 (3), pp. 353-372.

979 31. Govender, S.; Vadasz, P. Weak non-linear analysis of moderate Stefan number stationary convection in
980 rotating mushy layers. *Transport in Porous Media* **2002**, 49 (3), pp. 247-263.

981 32. Govender, S.; Vadasz, P., The effect of mechanical and thermal anisotropy on the stability of gravity
982 driven convection in rotating porous media in the presence of thermal non-equilibrium. *Transport in*
983 *Porous Media* **2007**, 69 (1), pp. 55-66.

984 33. Vadasz, P. On the evaluation of heat transfer and fluid flow by using the porous media approach with
985 application to cooling of electronic equipment. *Proceedings of the 5th Israeli Conference on Packaging of*
986 *Electronic Equipment*, Herzlia, Israel, 1991, pp. D.4.1-D.4.6.

987 34. Vadasz, P. Natural convection in rotating porous media induced by the centrifugal body force: The
988 solution for small aspect ratio. *ASME J. Energy Resources Technology* **1992**, 114, pp. 250-254.

989 35. Vadasz, P. Three-dimensional free convection in a long rotating porous box. *ASME J. Heat Transfer* **1993**,
990 115, pp. 639-644.

991 36. Vadasz, P. On Taylor-Proudman columns and geostrophic flow in rotating porous media. *SAIMechE*
992 *R&D Journal* **1994**, 10 (3), pp. 53-57.

993 37. Vadasz, P. Centrifugally generated free convection in a rotating porous box. *Int. J. Heat and Mass Transfer*
994 **1994**, 37 (16), pp. 2399-2404.

995 38. Vadasz, P. Stability of free convection in a narrow porous layer subject to rotation. *Int. Comm. Heat Mass*
996 *Transfer* **1994**, 21 (6), pp. 881-890.

997 39. Vadasz, P. Coriolis effect on free convection in a rotating porous box subject to uniform heat generation.
998 *Int. J. Heat and Mass Transfer* **1995**, 38 (11), pp. 2011-2018.

999 40. Vadasz, P. Stability of free convection in a rotating porous layer distant from the axis of rotation.
1000 *Transport in Porous Media* **1996**, 23, pp. 153-173.

1001 41. Vadasz, P. Convection and stability in a rotating porous layer with alternating direction of the centrifugal
1002 body force. *Int. J. Heat Mass Transfer* **1996**, 39 (8), pp. 1639-1647.

1003 42. Vadasz, P. Coriolis effect on gravity-driven convection in a rotating porous layer heated from below. *J.*
1004 *Fluid Mechanics* **1998**, 376, pp. 351-375.

1005 43. Vadasz, P.; Govender, S. Two-dimensional convection induced by gravity and centrifugal forces in a
1006 rotating porous layer far away from the axis of rotation. *Int. J. Rotating Machinery* **1998**, 4 (2), pp. 73-90.

1007 44. Vadasz, P.; Govender, S. Stability and stationary convection induced by gravity and centrifugal forces in
1008 a rotating porous layer distant from the axis of rotation. *Int. J. Engineering Science* **2001**, 39 (6), pp. 715-732.

1009 45. Vadasz, P.; Heerah, A. Experimental confirmation and analytical results of centrifugally-driven free
1010 convection in rotating porous media. *J. Porous Media* **1998**, 1 (3), pp. 261-272.

1011 46. Vadasz, P.; Olek, S. Transitions and chaos for free convection in a rotating porous layer. *Int. J. Heat Mass*
1012 *Transfer* **1998**, 41 (11), pp. 1417-1435.

1013 47. Bhaduria, B.S. Effect of temperature modulation on the onset of Darcy convection in a rotating porous
1014 medium. *Journal of Porous Media* **2008**, 11 (4), pp. 361-375.

1015 48. Malashetty, M.S.; Pop, I.; Heera, R. Linear and nonlinear double diffusive convection in a rotating
1016 sparsely packed porous layer using a thermal non-equilibrium model, *Continuum Mechanics and*
1017 *Thermodynamics* **2009**, 21 (4), pp. 317-339.

1018 49. Vanishree, R. K.; Siddheshwar, P. G. Effect of Rotation on Thermal Convection in an Anisotropic Porous
1019 Medium with Temperature-dependent Viscosity, *Transport in Porous Media* **2010**, 81 (1), pp.73-87.

1020 50. Agarwal, S.; Bhaduria, B.S.; Siddheshwar, P.G. Thermal instability of a nanofluid saturating a rotating
1021 anisotropic porous medium. *Special Topics & Reviews in Porous Media – An International Journal* **2011**, 2 (1),
1022 pp. 53-64.

1023 51. Bhaduria, B. S.; Siddheshwar, P. G.; Kumar, J.; Suthar, O.P. Weakly nonlinear stability analysis of
1024 temperature/gravity-modulated stationary Rayleigh–Bénard convection in a rotating porous medium,
1025 *Transport in Porous Media* **2012**, 92 (3), pp. 633-647.

1026 52. Agarwal, S.; Bhaduria, B.S. Flow patterns in linear state if Rayleigh-Benard convection in a rotating
1027 nanofluid layer. *Applied Nanoscience* **2014**, 4 (8), pp. 935-941.

1028 53. Malashetty, M.S.; Swamy, M.; Kulkarni, S. Thermal convection in a rotating porous layer using a thermal
1029 nonequilibrium model. *Physics of Fluids* **2007**, 19, pp. 054102/1-16.

1030 54. Malashetty, M.S.; Swamy, M. The effect of rotation on the onset of convection in a horizontal anisotropic
1031 porous layer. *Int. J. Thermal Sciences* **2007**, 46 (10), 1023–1032.

1032 55. Rana, P.; Agarwal, S. Convection in a binary nanofluid saturated rotating porous layer. *J. Nanofluids* **2015**,
1033 4, pp. 1-7.

1034 56. Yadav, D.; Lee, D.; Hee Cho, H.; Lee, J. The Onset of Double Diffusive Nanofluid Convection in a
1035 Rotating Porous Medium Layer with Thermal Conductivity and Viscosity Variation: A Revised Model, *J.*
1036 *Porous Media* **2016**, 19 (1), pp. 31-46.

1037 57. Rashidi, M.M.; Mohimanian Pour, S.A.; Hayat, T.; Obaidat, S. Analytic Approximate Solutions for Steady
1038 Flow over a Rotating Disk in Porous Medium with heat Transfer by Homotopy Analysis Method,
1039 *Computers & Fluids* **2012**, 54, pp. 1-9.

1040 58. Makinde, O.D.; Beg, O.A.; Takhar, H.S. Magnetohydrodynamic Viscous Flow in a Rotating Porous
1041 Medium Cylindrical Annulus with a Applied Radial Magnetic Field, *Int. J. Appl. Mathematics and*
1042 *Mechanics* **2009**, 5 (6), pp. 68-81.

1043 59. Straughan, B. *Stability and Wave Motion in Porous Media*. (Applied Mathematical Sciences Series 165),
1044 Springer, New York, 2008.

1045 60. Lombardo, S.; Mulone, G. Necessary and sufficient conditions of global nonlinear stability for rotating
1046 double-diffusive convection in a porous medium, *Continuum Mechanics and Thermodynamics* **2002**, 14 (6),
1047 pp. 527-540.

1048 61. Falsaperla, P.; Mulone, G.; Straughan, B. Rotating porous convection with Prescribed Heat Flux, *Int. J.*
1049 *Engineering Science* **2010**, 48 (7-8), pp. 685–692.

1050 62. Falsaperla, P.; Mulone, G.; Straughan, B. Inertia effects on rotating porous convection, *Int. J. Heat and Mass*
1051 *Transfer* **2011**, 54 (7-8), pp. 1352–1359.

1052 63. Falsaperla, P.; Giacobbe, A.; Mulone, G., Double Diffusion in Rotating Porous Media under General
1053 Boundary Conditions , *Int. J. Heat and Mass Transfer* **2012**, 55 (9-10), pp. 2412–2419.

1054 64. Capone, F.; De Luca, R. Ultimately boundedness and stability of triply diffusive mixtures in rotating
1055 porous layers under the action of Brinkman law. *Int. J. Non-Linear Mechanics* **2012**, 47 (7), pp. 799-805.

1056 65. Capone, F.; Rionero, S. Inertia effect on the onset of convection in rotating porous layers via the
1057 “auxiliary system method”. *Int. J. Non-Linear Mechanics* **2013**, 57, pp. 192-200.

1058 66. Capone, F.; De Luca, R. Coincidence between linear and global nonlinear stability of non-constant
1059 throughflows via the Rionero “Auxiliary System Method”. *Meccanica* **2014**, 49 (9), pp. 2025-2036.

1060 67. Boussinesq, J. *Theorie Analytique de la Chaleur*. 2, Gutheir-Villars, Paris, 1903, p. 172.

1061 68. Nield, D.A. The boundary correction for the Rayleigh-Darcy problem: limitations of the Brinkman
1062 equation. *J. Fluid Mechanics* **1983**, 128, pp. 37-46.

1063 69. Nield, D.A. The limitations of the Brinkman-Forchheimer equation in modeling flow in a saturated
1064 porous medium and at an interface. *Int. J. Heat and Fluid Flow* **1991**, 12 (3), pp. 269-272.

1065 70. Nield, D.A. Discussion on “Analysis of heat transfer regulation and modification employing
1066 intermittently emplaced porous cavities”. *J. Heat Transfer* **1995**, 117, pp. 554-555.

1067 71. Vafai, K.; Kim, S.J., Analysis of surface enhancement by a porous substrate. *ASME J. Heat Transfer* **1990**,
1068 112, pp. 700-706.

1069 72. Greenspan, H.P. *The Theory of Rotating Fluids*, Cambridge Univ. Press, Cambridge, 1980, pp. 5-18.

1070 73. Straughan, B. A sharp nonlinear stability threshold in rotating porous convection. *Proc. Royal Society of*
1071 *London A* **2001**, 457, pp. 87-93.

1072 74. Sheu, Long-Jye An autonomous system for chaotic convection in a porous medium using a thermal
1073 non-equilibrium model. *Chaos, Solitons & Fractals* **2006**, 30, pp. 672-689.

1074 75. Friedrich, R. The effect of Prandtl number on the cellular convection in a rotating fluid saturated porous
1075 medium. *ZAMM* **1983**, 63, pp. 246-249. (in German)

1076 76. Chandrasekhar, S. The instability of a layer of fluid heated from below and subject to Coriolis forces, *Proc. Royal Society of London A* **1953**, 217 (1130), pp. 306-327.

1077 77. Chandrasekhar, S. *Hydrodynamic and Hydromagnetic Stability*. Oxford Univ. Press, Oxford (1961), reprint by Dover Publications Inc., New York, 1981.

1078 78. Chakrabarti, A.; Gupta, A.S. Nonlinear thermohaline convection in a rotating porous medium. *Mechanics Research Communications* **1981**, 8 (1), pp. 9-22.

1079 79. Chand, R.; Rana, G.C. On the onset of thermal convection in rotating nanofluid layer saturating a Darcy-Brinkman porous medium, *Int. J. Heat and Mass Transfer* **2012**, 55, pp. 5417-5424.

1080 80. Capone, F.; Gentile, M. Sharp stability results in LTNE rotating anisotropic porous layer. *Int. J. Thermal Sciences* **2018**, 134, pp. 661-664.

1081 81. Galkwad, S.N.; Kouser, S. Analytical study of linear and nonlinear double diffusive convection in a rotating anisotropic porous layer with Soret effect. *J. Porous Media* **2012**, 12(8), pp. 745-761.

1082 82. Malashetty, M.S.; Heera, R. The effect of rotation on the onset of double diffusive convection in a horizontal anisotropic porous layer. *Transport in Porous Media* **2008**, 74, pp. 105-127.

1083 83. Malashetty, M.S.; Begum, I. The effect of rotation on the onset of double diffusive convection in a sparsely packed anisotropic porous layer. *Transport in Porous Media* **2011**, 88, pp. 315-345.

1084 84. Malashetty, M.S.; Kollur, P.; Sidram, W. Effect of rotation on the onset of double diffusive convection in a Darcy porous medium saturated with a couple stress fluid. *Applied Mathematical Modelling* **2013**, 37 (1-2), pp. 172-186. (The effect of rotation on the onset of double diffusive convection in a horizontal couple stress fluid-saturated porous layer, which is heated and salted from below, is studied analytically using both linear and weak nonlinear stability analyses. The extended Darcy model, which includes the time derivative and Coriolis terms, has been employed in the momentum equation. The onset criterion for stationary, oscillatory and finite amplitude convection is derived analytically. The effect of Taylor number, couple stress parameter, solute Rayleigh number, Lewis number, Darcy-Prandtl number, and normalized porosity on the stationary, oscillatory, and finite amplitude convection is shown graphically.)

1085 85. Kumar, A.; Bhaduria, B.S. Non-linear two dimensional double diffusive convection in a rotating porous layer saturated by a viscoelastic fluid. *Transport in Porous Media* **2011**, 87, pp. 229-250.

1086 86. Sunil; Sharma, A.; Bharti, P.K.; Shandil, R.G. Effect of rotation on a layer of micropolar ferromagnetic fluid heated from below saturating a porous medium. *Int. J. Engineering Sciences* **2006**, 44 (11-12), pp. 683-698.

1087 87. Bhaduria, B.S.; Agarwal, S. Natural convection in a nanofluid saturated rotating porous layer: a nonlinear study. *Transport in Porous Media* **2011**, 87, pp. 585-602.

1088 88. Yadav, D.; Lee, J. The effect of local thermal non-equilibrium on the onset of Brinkman convection in a nanofluid saturated rotating porous layer. *J. of Nanofluids* **2015**, 4 (3), pp. 335-342.

1089 89. Yadav, D.; Kim, M.C. The effect of rotation on the onset of transient Soret-driven buoyancy convection in a porous layer saturated by a nanofluid. *Microfluidics and Nanofluidics* **2014**, 17, pp. 1085-1093.

1090 90. Yadav, D.; Lee, J.; Cho, H.H. Brinkman convection induced by purely internal heating in a rotating porous medium layer saturated by a nanofluid. *Powder Technology* **2015**, 286, pp. 592-601.

1091 91. Yadav, D.; Bhargava, R.; Agrawal, G.S.; Yadav, N.; Lee, J., Kim, M.C. Thermal instability in a rotating porous layer saturated by a non-Newtonian nanofluid with thermal conductivity and viscosity variation. *Microfluidics and Nanofluidics* **2014**, 16, pp. 425-440.

1092 92. Yadav, D.; Wang, J.; Lee, J. Onset of Darcy-Brinkman convection in a rotating porous layer induced by purely internal heating. *J. Porous Media* **2017**, 20 (8), pp. 691-706.

1093 93. Malashetty, M.S.; Swamy, M. Combined effect of thermal modulation and rotation on the onset of stationary convection in a porous layer. *Transport in Porous Media* **2007**, 69, pp. 313-330.

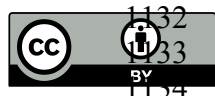
1094 94. Bhaduria, B.S. Fluid convection in a rotating porous layer under modulated temperature on the boundaries. *Transport in Porous Media* **2007**, 67, pp. 297-315.

1095 95. Om; Bhaduria, B.S.; Khan, A. modulated centrifugal convection in a vertical rotating porous layer distant from the axis of rotation. *Transport in Porous Media* **2009**, 79, pp. 255-264.

1096 96. Om; Bhaduria, B.S.; Khan, A. Rotating Brinkman-Lapwood convection with modulation. *Transport in Porous Media* **2011**, 88, pp. 369-383.

1097 97. Kang, J.; Niu, J.; Fu, C.; Tan, W. Coriolis effect on thermal convective instability of viscoelastic fluids in a rotating porous cylindrical annulus. *Transport in Porous Media* **2013**, 98, pp. 349-362.

1129 98. Rameshwar, Y.; Sultana, S.; Tagare, S.G. Küppers-Lortz instability in rotating Rayleigh-Benard convection
1130 in a porous medium, *Meccanica* **2013**, *48* (10), pp. 2401-2414.
1131



1132 © 2019 by the authors. Submitted for possible open access publication under the
1133 terms and conditions of the Creative Commons Attribution (CC BY) license
1134 (<http://creativecommons.org/licenses/by/4.0/>).